Technical Report

TR-98-25

Chemical processes causing cenetation in heta-affected smectite – the Kinnekulle bentonite

Roland Pusch
Geodevelopment AB, IDEON, Lund, Sweden

Hiroyasu Takase AB, Steven Benbow

Quantisci, Oxfordshire, United Kingdom

December 1998

Svensk Kärnbränslehantering AB
Swedish Nuclear Fuel
and Waste Management Co
Box 5864
SE-102 40 Stockholm Sweden
Tel 08-459 84 00
+46 8 459 84 00
Fax 08-661 57 19
+46 8 661 57 19

SKB

Chemical processes causing cementation in heat-affected smectite – the Kinnekulle bentonite

Roland Pusch
Geodevelopment AB, IDEON, Lund, Sweden

Hiroyasu Takase, Steven Benbow
Quantisci, Oxfordshire, United Kingdom

December 1998

PART 1

"CEMENTATION PROCESSES IN SMECTITE CLAY ASSOCIATED WITH CONVERSION OF SMECTITE TO ILLITE AS EXEMPLIFIED BY THE KINNEKULLE BENTONITES"

By ROLAND PUSCH

Geodevelopment AB, IDEON, 22 370 Lund, Sweden

ABSTRACT

Numerical calculation of silica migration and precipitation that can cause cementation of smectite buffer clay has been made using the Grindrod/Takase chemical model. It is used here to investigate whether the silicification of the bentonite and surrounding sediments at Kinnekulle, southwestern Sweden, can be explained by the heat pulse caused by the diabase intrusion that took place in Permian time.

Compilation of data concerning silica cementation and associated microstructural and rheological changes showed that significant silica precipitation should have occurred in the Kinnekulle case and this is also documented. Thus, precipitation of quartz has taken place to an extent that can be explained by the chemical model, which also showed conversion of smectite to illite by neoformation of the latter mineral but only for the 3000 years long heating period. Introduction of a criterion for non-reversible illitization is hence a necessary improvement of the model for explaining the actual presence of neoformed illite, which may in fact be wholly or partly responsible for the cementation.

SAMMANFATTNING

Numerisk beräkning av vandring och utfällning av kisel som kan orsaka cementering av smektitisk buffertlera har gjorts med användning av Grindrod/Takases kemiska modell. Den används här för att undersöka om silicificeringen av bentonit och omgivande sediment på Kinnekulle kan förklaras av värmepulsen vid inträngningen av permisk diabas.

Sammanställning av data rörande kiselcementering och samhöriga mikrostrukturella och reologiska förändringar visade att ansenlig kiselutfällning borde ha ägt rum i Kinnekullebentoniten och sådan dokumenteras också. Sålunda har utfällning av kvarts skett i den utsträckning som antyds av den kemiska modellen, som också visade omvandling av smektit genom nybildning av illit men endast under den 3000 år långa upphettningen. Införande av ett villkor för icke-reversibel illitisering är därför en nödvändig förbättring av modellen för att förklara existensen av nybildad illit, som i själva verket delvis eller helt kan förklara cementeringen.

LIST OF CONTENTS Page

SUMMARY

Earlier and present estimates suggest that conversion of smectite-rich buffer clay to non-expandable minerals like illite will not be a major threat to its isolating performance. Instead, cementation by precipitation of silica has been considered as a more critical process since it may reduce or eliminate the ductility and expandability of the clay. Numerical calculation of silica migration and precipitation has recently become possible by application of a chemical model proposed by Peter Grindrod and Hiroyasu Takase and it has been used in the present study to find our whether the silicification of the bentonite and surrounding sediments at Kinnekulle, southwestern Sweden, can be explained by the heat pulse caused by the diabase intrusion that took place in Permian time.

A compilation of experimental and geological data concerning silica cementation and associated microstructural and rheological changes forms the basis of the study. It showed that significant silica precipitation under chemically closed conditions does not take place at temperatures below about 130°C, implying that it should have occurred in the Kinnekulle case. In agreement with this, identification of cementing processes and agents and determination of their influence on the rheological properties of the Kinnekulle bentonite showed that precipitation of quartz has taken place to an extent that can be explained by the chemical model. The model also shows conversion of smectite to illite by neoformation of the latter mineral but only for the 3000 years long heating period. Better aggreement with the actual mineral composition would be obtained by introducing the criterion that illite formation is non-reversible. Neoformation of illite has been found by earlier investigators and it is proposed that this mineral may be wholly or partly responsible for the cementation.

1 SCOPE OF STUDY

Precipitation of dissolved matter in the porewater of buffer clay may be the most important degrading process in the clay. It can be caused by dissolution of smectite and accessory minerals in the hot part of the buffer, yielding free silica that can migrate towards the cold part where it precipitates. This process, which is driven by the concentration gradient generated by the temperature gradient, is manifested i.a. by the silicification of the Ordovician Kinnekulle bentonites. They offer a practical example of this process and will be used here for checking the applicability of the model of Reactive Chemical Transport worked out by Peter Grindrod and Hiroyasu Takase (Appendix).

2 BACKGROUND

2.1 EVIDENCE OF HEAT-INDUCED CHEMICAL CHANGES IN SMECTITE

2.1.1 Empirically deduced models

Precipitation of dissolved matter in the porewater of buffer clay is assumed to cause cementation that reduces the ability of the buffer to expand and self-heal. It may be caused by dissolution of smectite and accessory minerals in the hot part of the buffer, yielding free silica that migrates towards the cold part where it precipitates in the form of quartz, cristobalite or amorphous silica. Aluminum is expected to form complexes and be maintained where it is liberated.

Release of silica from smectite is commonly assumed to take place in conjunctionswith heat-induced conversion to illite (hydrous mica), [1,2]:

$$\text{Smectite} + K^{+} + Al^{3+} \longrightarrow \text{Illite} + Si^{4+} \qquad (2.1)$$

This process may have the form of replacement of tetrahedral silicons by aluminum ions supplied by dissolved minerals and potassium in the groundwater, or through neoformation of illite by synchronous crystallization of dissolved silica, aluminum and potassium. Both mechanisms yield silica that precipitates at reduced temperature. They are not unanimously proven by experiments or thermodynamically based geochemical codes but the following findings may be taken to support their validity.

2.1.2 Experimental

* Transmission electron microscopy of hydrothermally treated montmorillonite at temperatures from about 150-200°C showed precipitated 0.1-1 μm nodules of quartz and cristobalite and also of amorphous silica in the clay matrix [3]. Precipitated silica was estimated to make up about 1 % by weight. Coagulation of stacks of montmorillonite lamellae was found at 150°C and it was very obvious at 200°C.

* Transmission electron microscopy of hydrothermally treated montmorillonite at 200°C showed preciptated amorphous silica in the clay matrix representing about 1 % by weight [4]. Coagulation of stacks of lamellae was very strong.

* Transmission electron microscopy of hydrothermally treated montmorillonite at 150-200°C showed precipitated amorphous silica in the clay matrix at 200 °C representing about 1 % by weight [5]. Coagulation of stacks of montmorillonite lamellae was obvious at 150°C and strong at 200°C.

* Transmission electron microscopy, IR, and XRD were made on MX-80 samples one of which some was exposed to strong gamma radiation [6]. The 7 cm long samples saturated with very weakly brackish water were pressurized in cells (open system) for 1 year and heated to 90°C at one end and to 130°C at the opposite (temperature gradient 5.7°C/cm). The 130°C specimen showed a somewhat higher content of dense smectite aggregates than those representing lower temperatures, and precipitated gypsum and calcite were identified in this specimen and, to a less extent, in the 115°C specimen. Some minor amounts of quartz was also precipitated in the 90 and 115°C specimens but they were attributed to dissolution of feldspar.

* Transmission electron microscopy of autoclaved montmorillonite at 90-350°C showed precipitated amorphous silica in the clay matrix [7]. Coagulation of stacks of montmorillonite lamellae was obvious at 150°C and very strong at higher temperatures.

2.1.3 Geological evidence

* Mineralogical analysis by use of transmission electron microscopy of a profile comprising rhyolite/bentonite at Busachi, Sardinia, in which molten rock is concluded to have flowed and covered earlier formed bentonite, have given comprehensive microstructural and physical data [8]. Frequent 0.01-0.1 μm silica nodules were identified in the contact zone that had been heated to 500°C for 5 days and to 200°C for 2 months as evaluated from temperature calculations. Strong coagulation of stacks of montmorillonite lamellae had taken place as well. Where the temperature had not reached 150°C precipitations of silica could not be identified.

* Testing of bentonite drilling muds from depths representing temperatures of about 130°C shows considerable stiffening and appearance of lath-shaped neoformed illite and albite (personal communication by Prof. Necip Guven).

2.1.4 Conceptual models

Conceptual models describing the formation and nature of silica precipitations have been proposed [9,10,11]. Assuming the Edelman/Favejee crystal lattice model of montmorillonite to apply when Li- or Na-cations are present in interlamellar positions, heating to a critical temperature will cause collapse of the fraction of SiO_4 tetrahedrons that are inverted, by which Si is released [9]. The much stronger hydration of interlamellar Ca-ions implies that the lattice structure is of the traditional Endell/Hofmann/Wilm type and that such release of silica does not take place [10]. Silica accumulated in the interlamellar space in heated Na montmorillonite due to this process is illustrated in Figure 1 [11]. Figure 2 shows a conceptual model of silica precipitated at the edges of stacks of montmorillonite lamellae.

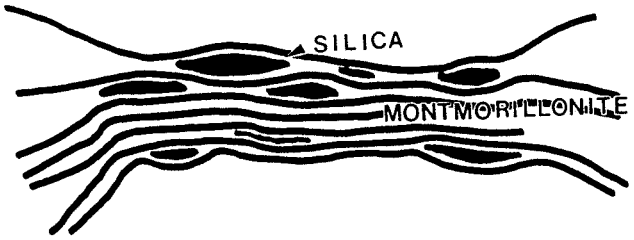

Figure 1. *Interlamellar precipitation of amorphous silica in heated montmorillonite [11].*

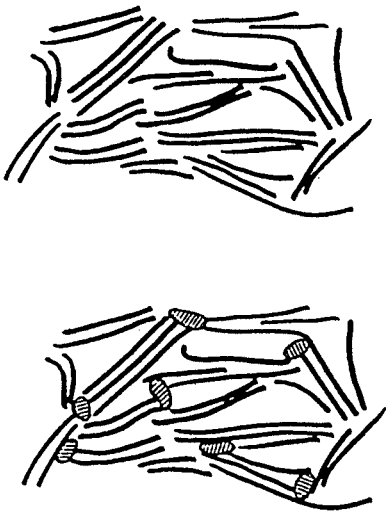

Figure 2. *Schematic view of silica precipitation at the edges of stacks of montmorillonite. Upper: Normal conditions. Lower: Silica precipitated connecting stacks and preventing them from expanding freely.*

2.1.5 Heat-induced rheological changes

Evidence

There is overwhelming evidence of very significant changes in the rheological behavior of Na bentonite exposed to heat under hydrothermal conditions [4,6,7,12].

* Fully water saturated MX-80 bentonite with a density of 1300 kg/m^3 autoclaved at 20, 105 and 150°C and then compressed uniaxially at room temperature showed almost the same stress/strain/time behavior with considerable creep (Figure 3), while samples autclaved at 200°C stiffened considerably and showed very little creep [4].

* MX-80 clay with a density at water saturation of 2050 kg/m^3 exposed for one year to 90-130 °C with and without gamma radiation showed only small changes when tested in a shear box [6]. However, the creep strain of the 130 °C was significantly smaller, i.e. about 50 % of that of unheated clay for a shear stress representing about 50 % of the shear strength.

* Montmorillonite clay autoclaved at temperatures from 25 to 250°C experienced the increase in shear strength at vane testing shown in Table 1 [7].

Table 1. *Viscosity and shear strength (yield point) of montmorillonite drilling fluid autoclaved at 25-250°C [7]. (6 % solid substance, distilled water).*

Temperature, °C	Viscosity, cp	Shear strength, lbs/100 sqft
25	15.5	9
150	35.5	21
200	73	66
250	88.5	79

* Systematic investigation of the shear strength of hydrothermally treated soft gels of MX-80 clay (1080 kg/m^3) was made by use of vane-testing in the Stripa Project for determining the longevity of clay grouts [12]. The outcome of long-term tests (270 days) with clay saturated with distilled water, strongly brackish (FF) and water with 50 % of the salinity of sea water (Sea/2), is summarized in Figure 4. For distilled water the highest strength was found for clay hydrothermally treated at 160°C, corresponding to about 2.5 times that of untreated clay. For the calcium-rich water the corresponding increase was about 3.5 times and for the sea-type water about 4 times. Strength testing of samples that had been treated at 200°C showed a drop in strength indicating dissolution and loss of material into the large water mass with which the clays were contacted via filters during the heat treatment. These tests show some slight strengthening already at 90°C while the most obvious effect was obtained for 130-160°C.

Tentative conclusions

All the rheological tests yield the same conclusion: Strengthening takes place but is small for temperatures below about 130°C. At 130-160°C considerable stiffening occurs and where no exchange of dissolved species takes place, as in autoclaved samples in closed cells, the shear strength increases with further increase in temperature (Figure 3, Table 1). Where chemical exchange with the surroundings occurs, significant dissolution and loss in peak strength may occur at higher temperatures (Figure 4).

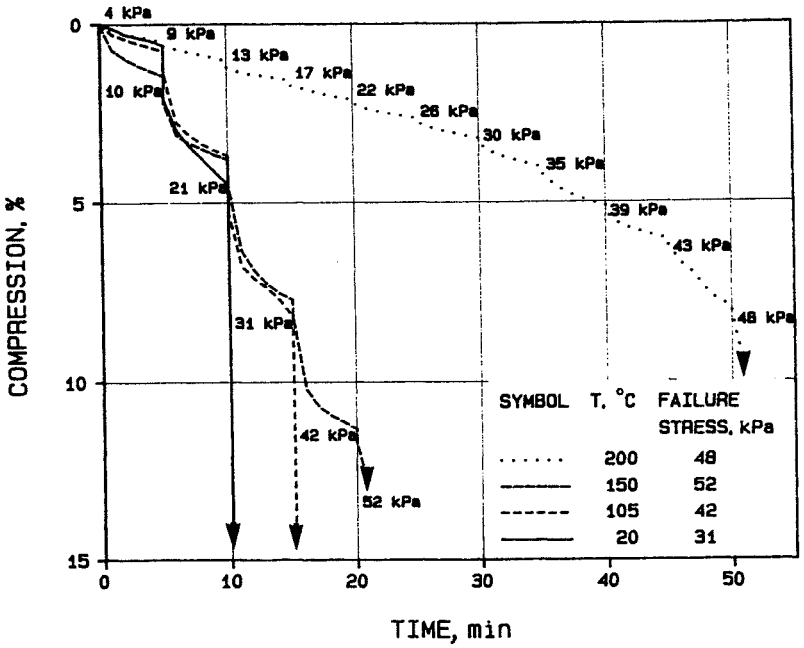

Figure 3. Axial compression versus time of autoclaved MX.80 [4].

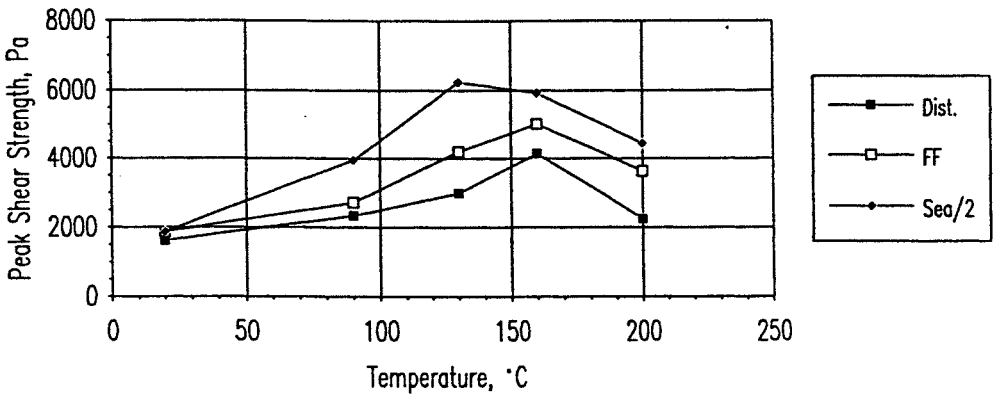

Figure 4. Shear strength of autoclaved soft Na bentonite gels [12].

2.1.6 General model

The overall conclusion from the hydrothermal, geological, rheological and theoretical investigations is that chemical changes that affect the rheological behavior of smectite clay are very small for temperatures lower than about 90°C, provided that only little chemical interaction with the surroundings takes place. The implies that the clay/water behaves as a closed system, which is a reasonable assumption for buffer clay in granitic environment.

For temperatures in the interval 90-130°C, heating of completely saturated dense smectite under hydrothermal conditions yields microstructural changes in the form of densification of aggregates of stacks of lamellae and an increase in bulk

strength, while no significant dissolution/precipitation of cementing agents takes place. Still, it is concluded that both quartz, sulphates and calcite precipitate, the two latter in the high-temperature part of smectite clay exposed to a temperature gradient. For temperatures exceeding 130°C, significant dissolution/precipitation is initiated together with stronger microstructural reorganization, and at 150-200°C it becomes important and causes brittleness and conversion to claystone.

In principle, the major heat-induced changes of hydrothermally treated smectite clay are concluded to be of the type illustrated in Figure 5.

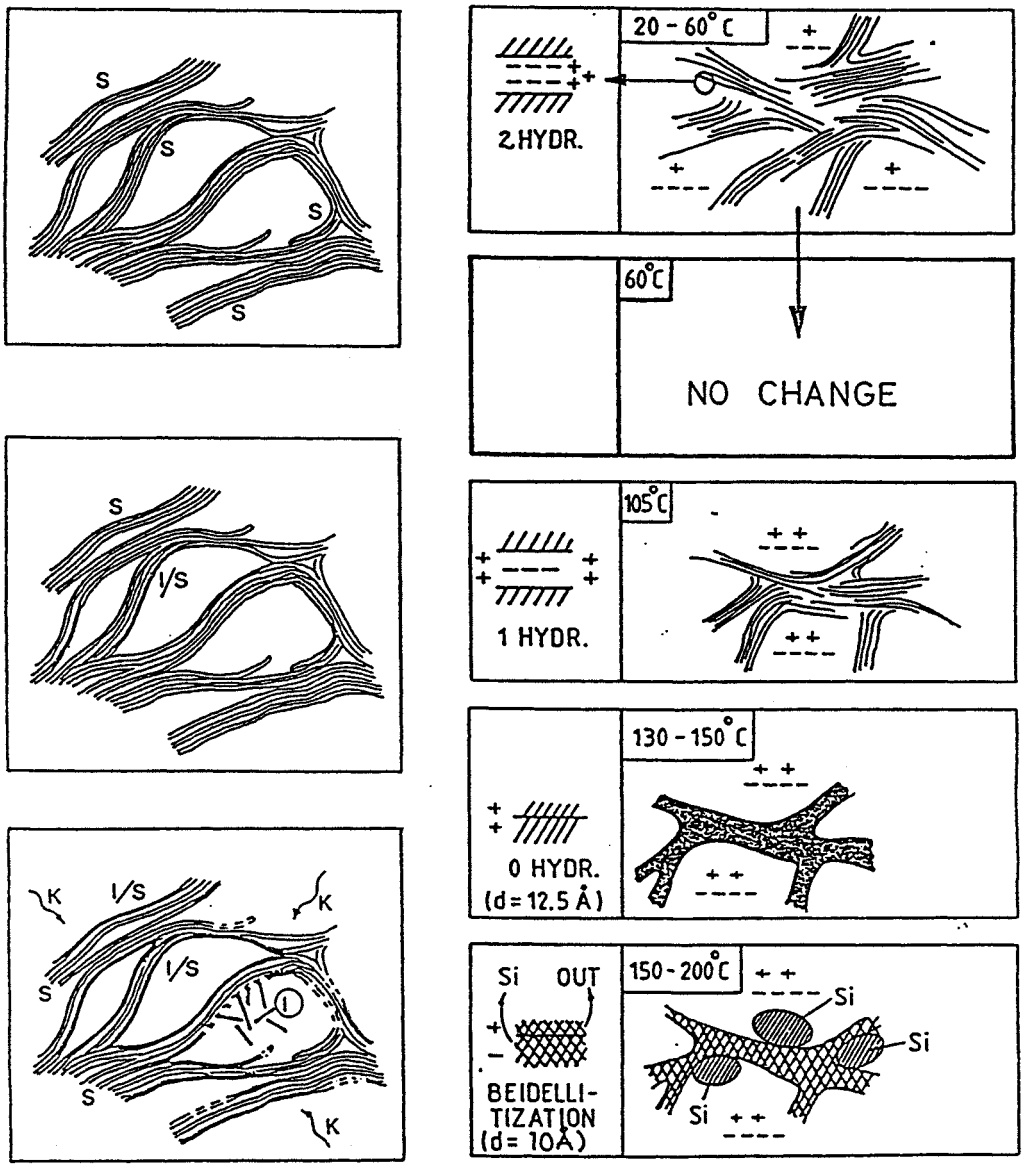

Figure 5. *Major features of smectite alteration model [12]. Left: Congruent dissolution, conversion of smectite (S) to illite (I). Right: Heat-induced coagulation of stacks of lamellae and precipitation of cementing quartz.*

3 THE KINNEKULLE CASE

3.1 SCOPE OF STUDY

The Kinnekulle sediment strata contain bentonite layers that have been exposed to a heat pulse by diabase intrusion in a fashion that resembles the one to which the clay buffer in a repository will be exposed. We will investigate here if the interpreted chemical changes, mainly silicification and associated conversion of smectite to illite, can be explained by the Grindrod/Takase model. For comparison, an earlier used version of conventional chemical models will also be used.

3.2 INTRODUCTION

The Chasmops series of Kinnekulle, some 150 km northeast of Gothenburg in southern Sweden, contains bentonite layers that have been the subject of a number of mineralogical investigations [13,14,15,16,17,18,19]. They led to somewhat different conclusions concerning the nature of the smectite-to illite conversion that is known to have taken place. Thus, Pusch & Madsen claimed, i.a. on the basis of Muller-Vonmoos' finding [18] that the smectite is of low-charge-type, that dissolution of smectite and accessory silicates gave neoformation of illite to an extent that was determined by the access to potassium. All the other, earlier models imply that the smectite lost silicons and formed beidellite that collapsed in conjunction with uptake and fixation of potassium. Both concepts imply that silica is released from degrading smectite and is free to migrate within and from the buffer. The major difference between the two concepts is that aluminum according to the model of Pusch and Madsen appears in ionic form in the porewater where it contributes to the neofomation of illite, while it stays intracrystalline according to the other concepts.

3.3 FORMATION

3.3.1 Stratigraphy

The general stratigraphy of the Kinnekulle hill area is shown in Figure 6. Diabase (basalt) of Permian age forms the top of the about 200 m thick series of shales, limestones and sandstones that rest on the crystalline bedrock. At about 95 m depth below the diabase cap bentonite layers are present, among which there is an approximately 2 m thick bed and two decimeter-thick layers within 1 m distance above the thick bed and three 0.1-0.2 m thick layers within 2.5 m distance below the base of the thick bed. Figure 7 shows the sediment profile at the level where the thick bed, which was in focus of the present study, is located.

3.3.2 Evolution

Volcanic ash was deposited in seawater on top of about 120 m of muds and calcareous sediments in the Kinnekulle area in southwestern Sweden about 450 M years ago. Additional sediments of similar type and also quartz-rich silty and sandy soils were then deposited on top of the ash, yielding an overlying several hundred hundred meters thick series of marine sediements. The ash originated from rhyolite or dacite lava and was converted to smectitic bentonite layers that were consolidated under an effective pressure of 5-10 MPa, yielding a density of 2000-2200 kg/m^3 and a porosity of 30-40 %.

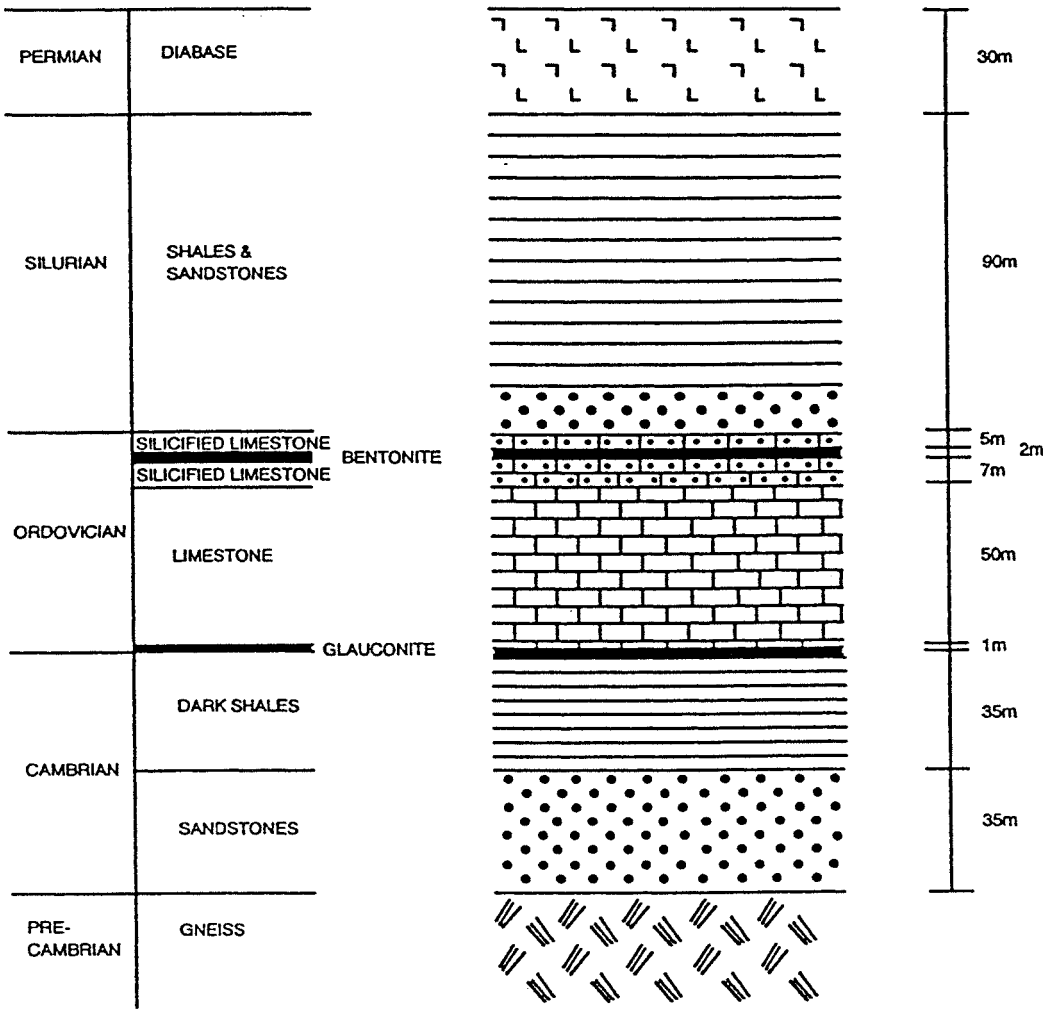

Figure 6. *The Kinnekulle strata [8,19].*

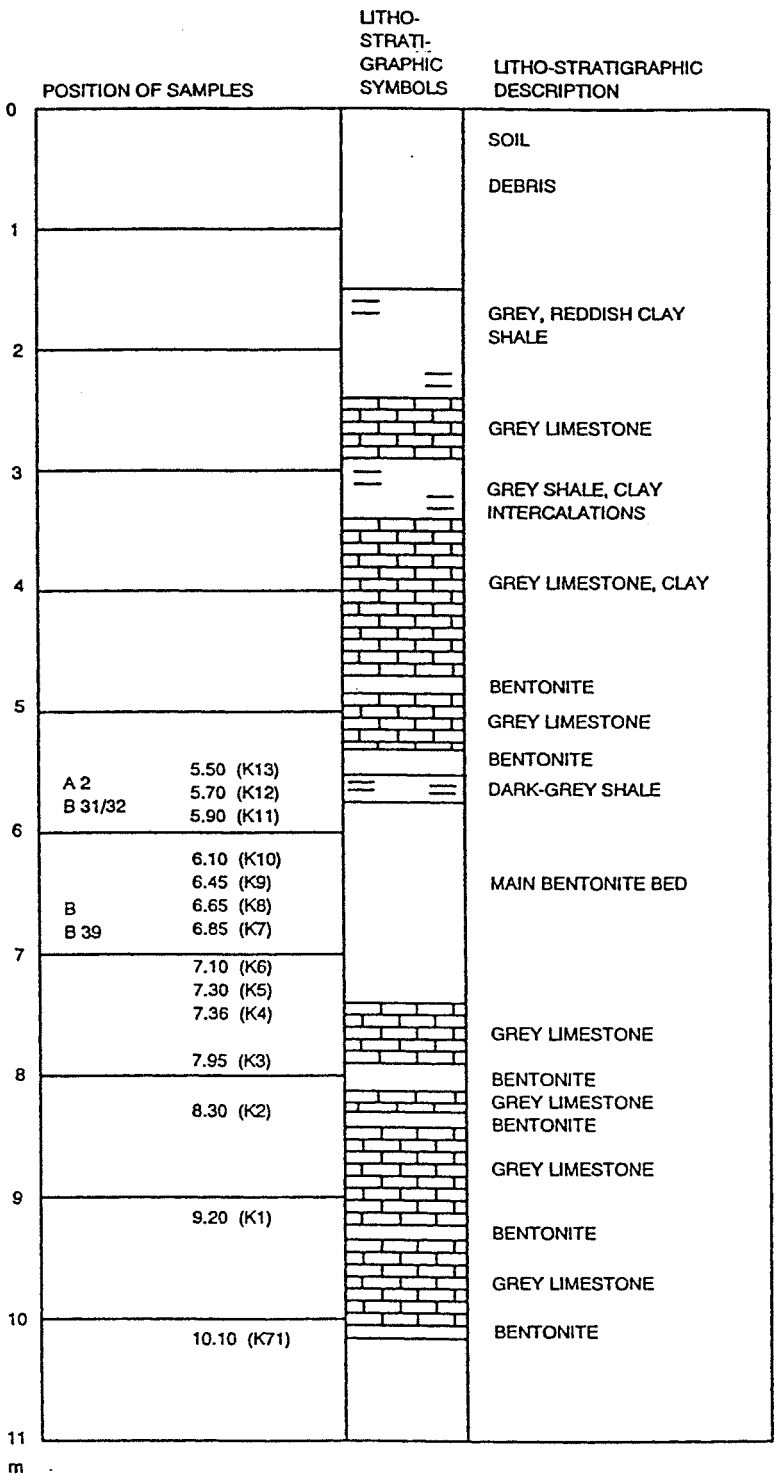

Figure 7. *Detailed stratigraphy at the level of the 2m thick bentonite bed.[9,19].*

About 300 M years ago magma moved up locally through the sediment series and penetrated laterally into it, forming a diabase (basalt) layer with a thickness of several tens of meters. It exposed the sediments to heat that reached down to the bentonite layers where it caused illitization and silicification.

Prequaternary erosion and Quaternary glaciation removed part of the diabase layer and the overlying sediments. The maximum overburden pressure is concluded to have been about 30 MPa in Quaternary time, yielding a probable water content of about 15 %. The present water content is 22-35 % of the 2 m thick bentonite bed, indicating expansion due to the unloading to the very low present overburden pressure 0.1 MPa. It should in fact have been somewhat more if the clay had retained its expandability and the discrepancy is attributed to cementation preventing the smectite to expand freely.

3.3.3 Temperature history

The temperature evolution has been derived by use of conodont analysis and thermal numerical calculations assuming the initial temperature of the diabase magma to be 1100°C and applying reasonable thermal properties of the sediment series. The derived temperature evolution is shown in Figure 8. The maximum temperature is estimated to have been 140°C and the average temperature about 130°C for a couple of hundred years. After 1000 years the temperature is assumed to have been 60-90°C for 1000 years and 30-60°C for the subsequent 1000 years. The peak temperature may in fact have been as high as 160°C but it is conservatively taken as shown in the diagram.

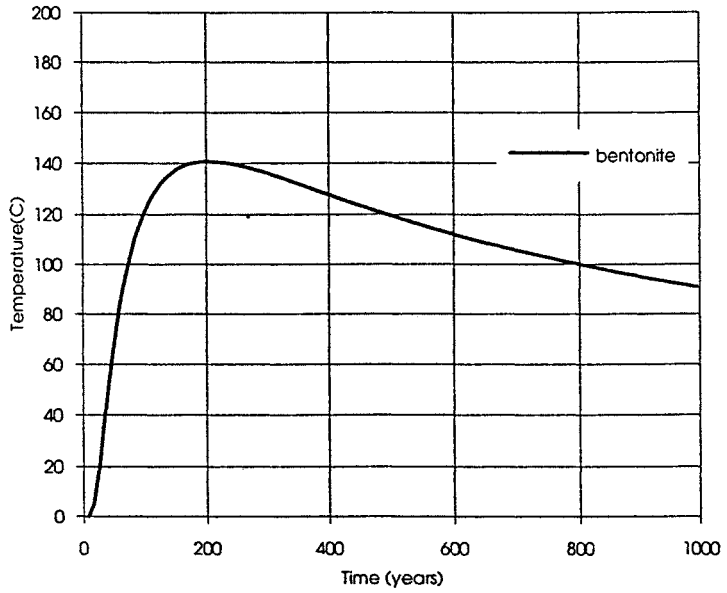

Figure 8. *Temperature in bentonite beds in the first 1000 years after the magma intrusion.*

The temperature gradient existing across the 2 m bentonite bed is assumed to be the driving force of the silicification. It varied according to Figure 9 in the first 1000 years and hence never exceeded 0.05°C/cm.

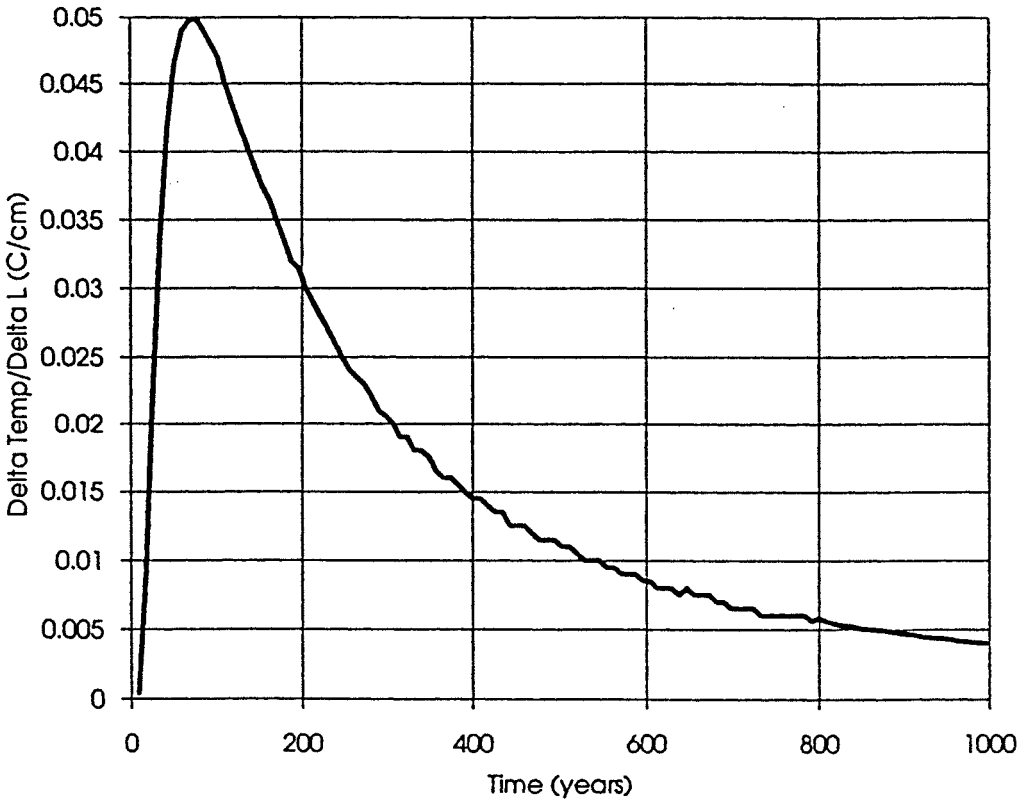

Figure 9. *Temperature gradient in the 2 m thick bentonite bed.*

3.4 MINERALOGY

Quartz is the most abundant phenocryst species, forming 30-40 % of the total mineral content. Silica in amorphous form represents about 0.5 % of the total mineral content.

Clay minerals appear in the clay fraction, which forms 35-40 % of the solid phase. They are predominantly illite (I) and smectite (S) and appear separately or as mixed layer minerals. There is a variation in illite content that indicates that illitization was initiated at the upper and lower boundaries of the thick bentonite bed, i.e. from where potassium could enter (Table 1), and proceeded into the bed.

For samples K8 (center of the 2 m bed) and K12 (uppermost part of the 2 m bed) the content of separate smectite (S) in the form of montmorillonite and I/S in the clay fraction is estimated at 60 % and 45 %, respectively. These figures correspond to about 25 and 18 weight percent of the total mineral content. The most interesting data in the present context concern the I/S ratio of the clay fraction, which is estimated at 0.65 for the uppermost part of the bed and 0.45 for its central part. The actual content of pure smectite expressed in weight percent of the total mineral content is about 8 % in the firstmentioned upper part and 25 % in the center of the bed.

Table 1. *Mineral content in the <1 μm fraction*

Position in Figure 7	Illite fraction of Illite/smectite	
5.70 m (K10/K12)	41-65 % I in I/S	5-8 % quartz
6.45 m (K9)	37-54 % I in I/S	5 % quartz
6.85 m (K7/K8)	36-51 % I in I/S	3 % quartz

3.5 INDICATIONS OF SILICIFICATION

3.5.1 Microscopy

SEM pictures show that silica in the form of quartz, cristobalite and amorphous silica appear as 2-5 μm objects precipitated on flaky rock-forming minerals and as smaller ones on smectite stacks (Figure 10).

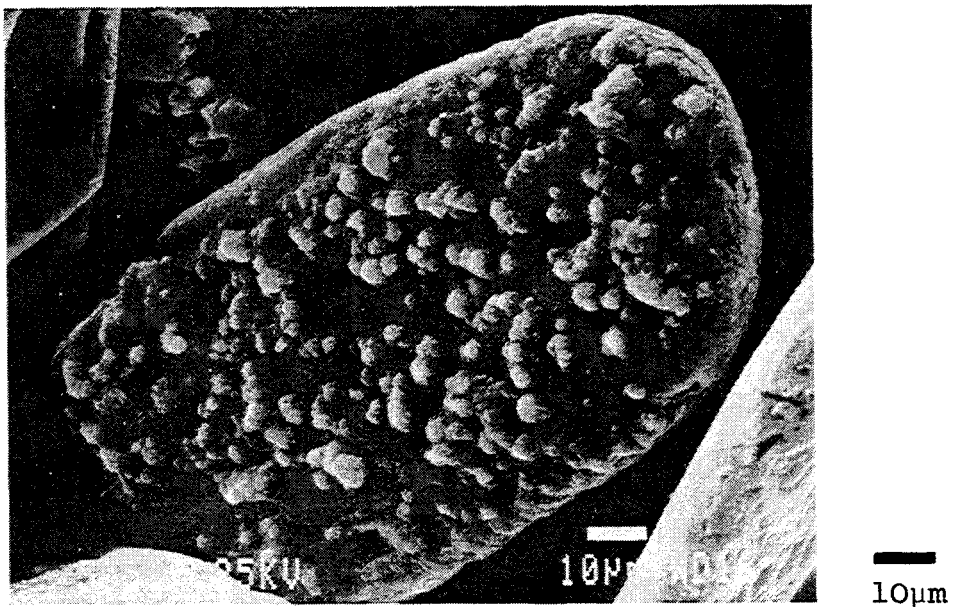

Figure 10. *Silica precipitated on silt particle in the 2 m bentonite bed [18].*

3.5.2 Grain size distribution

Ultrasonic treatment of samples from the 2 m bentonite bed has been found to increase the content of minus 2 μm particles from about 12 % to about 55 % and to decrease the content of particles larger than 63 μm from 65 % to 2 % [18]. This effect is ascribed to breakage of cementitious bonds.

3.5.3 Physical properties

Swelling pressure tests have been made on sample K8 (center of 2 m bed) and K12 (uppermost part of 2 m bed). For the same density at water saturation, 2100 kg/m^3, the swelling pressure of K8 was found to be 15 MPa, while that of K12 was 3.8 MPa [18]. The difference means that the K12 sample swelled significantly less than the K8 sample despite the relatively small difference in expandables (45 and 60 %, respectively). This can be explained by more cementation at the K12 level, for which quartz precipitation may be responsible as indicated by the higher quartz content in K12 (about 6 %), while this content is significantly lower (around 3 %) in K8, representing the center of the bed.

Shearing of an undisturbed sample that had a bulk density at saturation of 1850 kg/m^3 by use of a shear box gave a shear strength of 300 kPa [19], i.e. about twice the shear strength of MX-80 clay with this density, showed that log time creep strain was characteristic of all the load steps except, as expected, the one yielding failure. The stress/time curves were all irregular and discontinuous, which can be explained by microstructural breakdown in the form of successively fractured cementation bonds. The fact that the clay sustained rather large strain before failure took place indicates that only part of the strength-producing components caused by cementing bonds were mobilized initially, while activation of smectite aggregates occurred subsequently, providing new bonds in a "self-healing" process. This indicates that slight cementation of the buffer clay in a KBS3 repository may not be very critical since strain-induced reactivation of the clay matrix may generate the required sealing ability.

4 CHEMICAL MODELS

4.1 GENERAL

Up til now modeling of heat-induced chemical changes in the Kinnekulle bentonite series has only been made with respect to the partial conversion of the original smectite content to illite that is known to have taken place. One example of this sort of calculation, which represents convential ways of treating the matter and which was performed by Pusch and Madsen [20], is cited here. This chapter also summarizes an attempt of chemical modeling made by Takase and Benbow, which is added as an appendix to this report, and which comprises the silicification that is thought to be associated with the smectite-to-illite conversion.

4.2 PUSCH/MADSEN MODELING

4.2.1 Assumptions

The smectite-to-illite conversion model proposed by Pytte & Reynolds in 1989 [21] forms the basis for the calculation of the Kinnekulle event performed by Pusch & Madsen in 1995 [20]. They assumed that the K/Na ratio in the system remained constant throughout the conversion period and they applied the *f*- and *g*-functions of the general expression for the rate of change of the smectite content:

$$-dS/dt = Ae^{-U/RT} f(K^+/Na^+) g(S) \qquad (4\text{-}1)$$

where:
A = Constant
U = Activation energy
K^+ and Na^+ = Potassium and sodium concentrations (f is function of them)
S = Mole fraction of smectite in I/S
g = Function of semctite concentration in I/S
R = Universal gas constant
T = Temperature

The K^+ concentration in the porewater was taken to be 0.01 moles per liter, corresponding to the potassium concentration in seawater. Ca^{2+} was not considered.

4.2.2 Results

Calculations applying the activation energies 25 and 27 kcal/mole showed that the lower energy yields an I/S value of about 0.65, which is on the right order of magnitue. The higher activation energy would bring I/S down to 0.15. However,

if the temperature had been higher than calculated, a higher activation energy may have given the same I/S ratio, which shows that the model is very sensitive to the selection of input data. This is obvious from the diagrams in Figure 11, which give the calculated rate of smectite conversion for K^+=0.01 mole/liter and U=25 kcal/mole and the corresponding conversion rate for K^+=0.05 mole/liter and U=27 kcal/mole.

The authors concluded that the migration of K^+ was the key rate factor and that the conversion to illite to the present extent would have required faster migration of potassium to the reaction zone than simple diffusion can offer. They also suggested, referring to the significant amount of well crystallized minute illite particles (Figure 12), that neoformation of illite is much more probable than solid state conversion, and also that the illite particles may serve as cement, meaning that precipitation of quartz may not be the major silicification process.

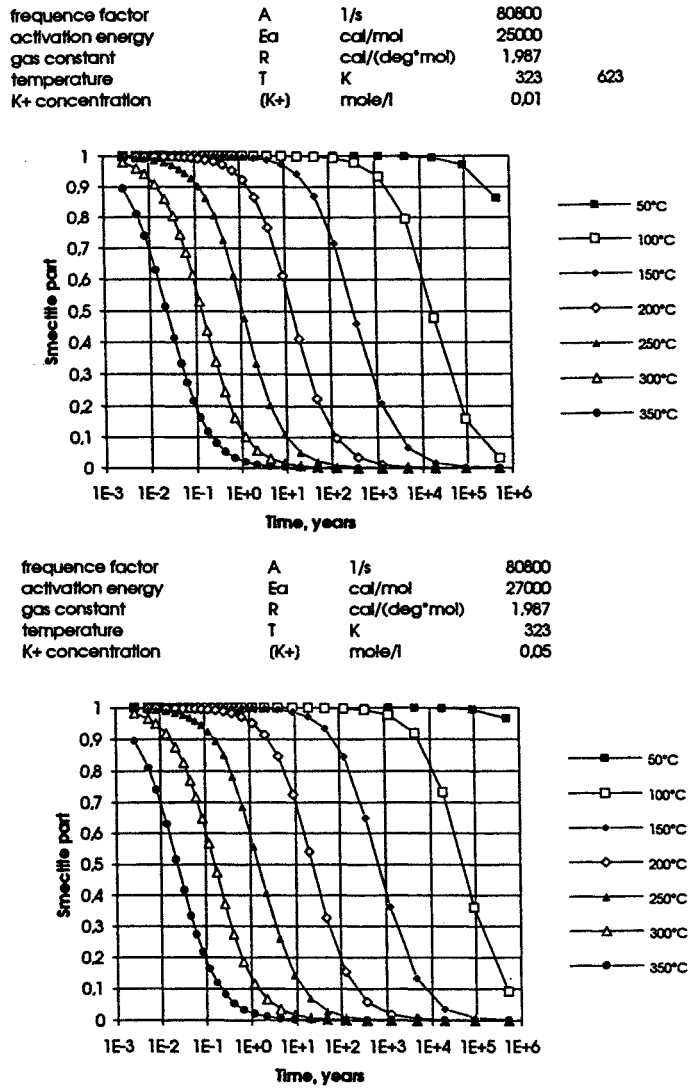

Figure 11. *Rate of conversion of smectite calculated by Pytte/Reynold's model. Scale: Vertical axis is proportion of smectite (1=100 %), Horizontal gives log time from 0.001 (1E-3) to 1 million (1E+6) years. Upper: Activation energy 25 kcal/mole and K^+=0.01 mole. Lower: Activation energy 27 kcal/mole and K^+=0.05 mole.*

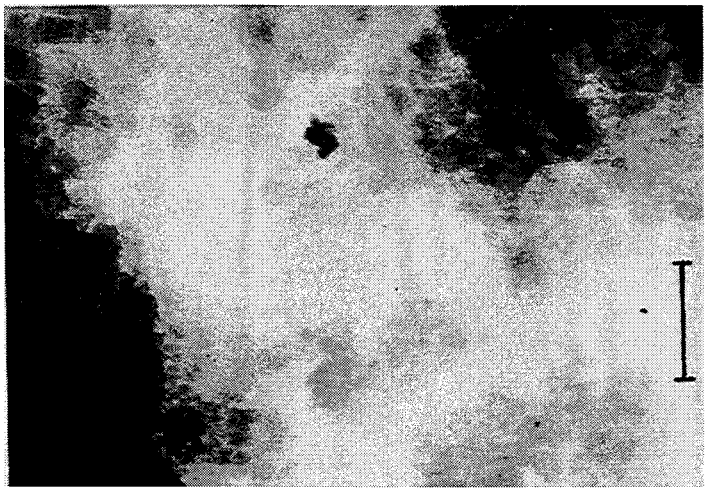

Figure 12. *Transmission electron micrograph of dispersed Kinnekulle bentonite. Numerous particles with a maximum diameter of 0.01-0.05 μm can be seen. Scale is 0.1 μm.*

4.3 TAKASE/BENBOW MODELING

Calculation of chemical processes in the 2 m thick Kinnekulle bentonite bed was made by Takase and Benbow using the model proposed by Takase and Grindrod [22]. The complete calculations are given as an appendix to the present report.

4.3.1 Assumptions

The reaction system was simplified to consist of temperature-dependent amounts of smectite, illite, silica [$SiO_{2(aq)}$], potassium (K^+), and aluminum [Al, $Al(OH)_4^-$, while the concentrations of H^+, Na^+, and Mg^{2+} were taken to be constant and equal to those in seawater.

The outer boundaries of the reaction system were located at 10 m distance from the upper and lower surfaces of the 2 m thick bentonite bed.

4.3.2 Models

Two models were tried for calculating the alteration of smectite to illite: 1) solid state conversion, and 2) smectite dissolution and neoformation of illite.

Solid state conversion

The assumed reaction comprised illitization by uptake of K^+ and Al^{3+} of the smectite and release of silica in the form of SiO_2. It was formulated as an Arrhenius function with the activation energies 24 and 28 kcal/mole, respectively.

Smectite dissolution and neoformation of illite

The assumed reaction was dissolution of smectite and precipitation of neoformed illite. For the reaction rate an empirical expression with the specific surface area as one component was employed. The silica compounds quartz and amorphous silica were also modeled using empirical kinetic and equilibrium constants.

Since the rate of neoformation of illite and silicious compounds depend on how fast dissolved species migrate, the diffusivity was introduced in the calculations.

4.3.3 Results

Basis for comparison

Comparison was made between the actually recorded conversion of smectie and precipitation of quartz. The assumed initial content of smectite (montmorillonite) of the 2 m thick bed was 75 % by weight while the initial illite and quartz contents were 0 and 25 %, respectively. The average actual illite content of the uppermost part of the bed is presently 55 % while the total quartz content is about 35 %. The quartz content in the clay fraction, i.e. where precipitated quartz is expected to appear, is 6 %. In the central part of the bed the corresponding figures are 45 and 3 %, respectively.

The solid state conversion model

The solid state conversion model gave an amount of illite after 3000 years that was very small, i.e. 0.012 % by weight for the activation energy 28 kcal/mole and 0.6 % for 24 kcal/mole. The associated release of silica that could migrate and be precipitated was found to be vanishingly small according to the model, which hence does not apply to the Kinnekulle case. However, the calculated tendency of stronger illitization in the peripheral parts than in the central part of the bed is in agreement with the real conditions.

The dissolution/precipitation model

The smectite dissolution model gave amounts of illite in the hottest period that were in better agreement with the presently recorded ones. Thus, 20 % by weight of the smectite would be altered to illite within 0.5 m distance from the upper end of the bed while about 7 % would have turned into illite in the central part of the bed. Within 0.1 m distance from the upper and lower ends of the bed, 36-44 % of the smectite would have been converted to illite, which is not too different from the actual percentages. Although the figures are lower than the actual ones, they still indicate that the model and assumptions are relevant, but they have to be questioned since the calculated changes only refer to the hottest period and turn out to be much smaller at the end of the 3000 year period when the temperature has dropped back to normal again.

As to silicification, the model seems to yield almost the actual quartz contents (increase of total quartz content from assumed 25 % to about 31 %) and the resulting very minor amount of amorphous silica is also in agreement with what has actually been recorded.

In order to improve the model to yield adequate data the authors made an attempt to couple the smectite dissolution to irreversible illite formation. This approach, which is scientifically sound, still gave very small amounts of neoformed illite, even when the activation energy for dissolution was taken as low as 15 kcal/mole. The authors suggested that since the calculated illite formation was confined to the close vicinity of the upper and lower boundaries of the bed, the access to potassium was concluded to have been a rate-limiting factor.

5 DISCUSSION AND CONCLUSIONS

5.1 CHEMICAL PROCESSES

Compilation of experimental data from hydrothermally treated smectite and from relevant geological examples show that temperature is the most important factor for chemical conversion that can jeopardize the sealing function of buffer clay with montmorillonite as major smectite species. The following changes, referring to smectite-rich buffer produced by compaction of bentonite granules, may take place in different temperature regions:

1. In the interval up to 60°C there will be no significant changes in composition, microstructure and rheology even in a very long time perspective.

2. In the interval 60-90°C small microstructural changes take place primarily in the form of homogenization of the clay due to breakdown of grains (granules) by thermally induced stresses. Significant dissolution of smectite and other silicates is initiated and illitization begins at a rate that is controlled by the access to potassium. In a 3000 year perspective with constant access to potassium corresponding to the concentration in seawater, the illitization in buffer clay is expected to be less than 10 %.

3. In the interval 90-130°C dense aggregates appear to undergo compression and there is a general tendency towards coagulation. More significant dissolution of smectite and other silicates takes place and the illitization rate is increased but the access to potassium is a controlling factor. In a 3000 year perspective the illitization in open systems like the Kinnekulle bentonite may be several tens of percent but in closed systems, which buffer clay resembles, the formation of illite may still be very limited in a 3000 year perspective if the potassium supply is small as when the tunnel backfill is poor in soluble potassium, and if groundwater flow in the nearfield is very limited.

4. At higher temperatures than 130-150°C dissolution of smectite and other silicates increases very much and precipitation of silica at cooling is comprehensive. Transformation to claystone is initiated.

5.2 MODELING

The conventional Reynold-type models do not offer a possibility to predict chemical changes since the basic reaction is preset to be smectite-to-illite conversion and release of silica. They can be forced to give reasonable data by introducing parameter values that are obtained by back-calculations but they are not able to predict the nature of the illite or the precipitated silica.

The Takase/Benbow modeling, based on the Takase/Grindrod model, may offer a better possibility to describe and predict the extent of illitization and quartz

precipitation if it is further developed and includes the concept of irreversible illite formation. At present it is of limited use.

As in many other contexts it is necessary to base mathematical models on true conceptual models, which, in the present case, requires that much more detailed microstructural and microchemical analyses be made on smectitic clay exposed to relevant and well defined hydrothermal conditions. It appears that the planned Äspö Prototype experiments would offer this possibility.

5.3 GENERAL REMARK

Despite the chemical alteration of the Kinnekulle bentonite bed it must be underlined that the ductility and expandability of this very old smectite clay with temperature and stress histories that are similar to those of the forthcoming buffer in a KBS3 repository, certainly offer a very good example of the long term performance of this sort of clay.

6 REFERENCES

1. **Perry A E, Hower J**, 1970. Burial diagenesis in Gulf Coast pelitic sediments. Clays Clay Minerals, Vol.18 (pp.165-177).

2. **Hower J, Eslinger E V, Hower M, Perry A E**, 1976. Mechanisms of burial metamorphism of argillaceous sediment: Mineralogical and chemical evidence. Geol. Soc. Am. Bull., Vol.87 (pp.725-737).

3. **Pusch R**, 1987. Permanent crystal lattice contraction, a primary mechanism in thermally induced alteration of Na bentonite. Scientific Basis for Nuclear Waste Management X (J K Bates and W B Seefeldt, editors). Mat. Res. Soc. Symp. Proc., Vol.84, Boston (pp. 791-802).

4. **Pusch R, Touret O**, 1987. Heat effects on soft Na bentonite clay gels. Geologiska Föreningens i Stockholm Förhandlingar, Vol.110 (pp. 183-190).

5. **Pusch R, Guven N**, 1990. Electron microscopic examination of hydrothermally treated bentonite clay. Engineering Geology, Vol.28 (pp. 303-314).

6. **Pusch R, Karnland O, Lajudie A, Decarreau A**, 1993. MX-80 clay exposed to high temperatures and gamma radiation. SKB Technical Report TR 93-03, SKB, Stockholm.

7. **Guven N, Carney L L, Malekahmadi F, Lee L J**, 1984. Factors affecting the behavior of bentonite fluids and their in-situ conversion into cement, Final Report. Sandia Nat. Laboratories, Contractor Report SAND84-7170, UC-66c University of California.

8. **Pusch R, Karnland O**, 1988. Geological evidence of smectite longevity. The Sardinian and Gotland cases. SKB Technical Report TR 88-26, SKB, Stockholm.

9. **Pusch R**, 1983. Stability of deep-sited smectite minerals in crystalline rock - chemical aspects. SKBF/KBS Technical Report TR 83-16, SKB, Stockholm.

10. **Pusch R, 1993**. Evolution of models for conversion of smectite to non-expandable minerals. SKB Technical Report TR 93-33. SKB, Stockholm.

11. **Meike A**, 1988. Transmission electron microscopy of hydrothermally altered bentonites. Internal Report Earth Sciences Board. University of California at Santa Cruz.

12. **Pusch R, Karnland O, Hökmark H, Sanden T, Börgesson L**, 1991. Final Report of the Rock Sealing Project - Sealing properties and longevity of

smectitic clay grouts. Stripa Project Technical Report TR 91-30, SKB, Stockholm.

13. **Thorslund P**, 1945. Om bentonitlager i Sveriges kanbrosilur. Geologiska Föreningens i Stockholm Förhandlingar, Vol.67 (p.286).

14. **Byström A.M**, 1956. Mineralogy of the Ordovician bentonite beds at Kinnekulle, Sweden. Swedish Geological Survey, Ser, C. No.540, Stockholm.

15.**Velde B, Brusewitz, A.M**, 1982. Metasomatic and non-metasomatic low-grade metamorphism of Ordovician meta-bentonites in Sweden. Geochim. Cosmochim. Acta, Vol.46 (pp.447-452).

16. **Brusewitz A.M**, 1986. Chemical and physical properties of Paleozoic bentonites from Kinnekulle, Sweden. Clays and Clay Minerals, Vol.34, No.4 (pp.442-454)

17. **Inoue A, Watanabe T, Kohyama N, Brusewitz A.M**, 1990. Characterization of illitization of smectite in bentonite beds at Kinnekullle. Clays and Clay Minerals, Vol.38, No.3 (pp. 241-249).

18. **MullerVonmooos M, Kahr G, Bucher F, Madsen F T**, 1994. Intracrystalline swelling of mixed-layer illite/smectite in K-bentonites. Engineering Geology, Vol. 28, No..3-4.

19. **Pusch R, Börgesson L, Erlström M**, 1987. Alteration of isolating properties of dense smectite clay in repository environment as exemplified by seven prequaternary clays. SKB Technical Report TR 87-29.

20. **Pusch R, Madsen F T**, 1995. Aspects of the illitization of the Kinnekulle bentonites. Clays and Clay Minerals, Vol.43, No.3 (pp.261-270).

21. **Pytte A M, Reynolds R C**, 1989. The thermal transformation of smectite to illite. In Thermal History of Sedimentary Basins; N D Naeser and T H McCulloh, eds, Springer-Verlag, New York (pp.133-140).

22. **Grindrod P, Takase H**, 1994. Reactive Chemical Transport within engineered barriers. 4th Int. Conf. Chemistry and Migration Behaviour of Actinides and Fission Products in the Geosphere. R. Oldenburg Verlag, Munchen.

PART 2

"NONISOTHERMAL MODELLING OF GEOCHEMICAL EVOLUTION IN THE KINNEKULLE BENTONITE LAYER"

By HIROYASU TAKASE and STEVEN BENBOW

QuantiSci Chiltern House, 45 Station road, Henley on Thames, Oxfordshire, RG9 1 AT United Kingdom

Nonisothermal modelling of geochemical evolution in the Kinnekulle bentonite layer

- Mathematical modelling and simulation -

Hiroyasu Takase
Steven Benbow

QuantiSci

Chiltern House, 45 Station Road, Henley on Thames,
Oxforshire, RG9 1AT theUnited Kingdom.

1. Introduction

450 million years ago, volcanic ash was deposited in sea water on the top of mud and calcareous sediments in Kinnekulle area in south-western Sweden. Additional sediments of similar type and also quartz-rich soil were then deposited over the ash, yielding an overlying series of marine sediments whose thickness is several hundred metres. The ash was originated from rhyolite or dacite lava and converted to smectite layers.

About 300 million years ago, magma moved up locally through the sediment series and penetrated laterally into it, forming a basalt layer with a thickness of several tens of meters. It exposed the sediments to heat that reached down to the bentonite layers where it caused illitization and silicification. The temperature at the centre of the 2 m thick bentonite layer reached its peak, 140 C°, around two hundred years after the magmatic intrusion, and stayed above 100 C° for 600 years after that. The temperature gradient across the bentonite layer went up to 5 C°/m 70 years after intrusion and gradually went down below 1 C°/m in the next 400 years or so. After 1,000 years the temperature is assumed to have been 60 - 90 C° and 30 - 60 C° for the subsequent 1,000 years. The influence of temperature on the silicification after the first 1,000 years is considered to be very small [**1**].

The current mineralogy in the bentonite layer can be summarised as follows:

1. Quartz is the most abundant phenocryst species, forming 30 - 40 % of the total mineral content. Silica in amorphous form represents about 0.5 % of the total mineral content.

2. Clay minerals form 35 - 40 % of the solid phase. It consists mainly of mixed-layer illite-smectite (I/S) clays and also contains montmorillonite, illite and chlorite. The content of montmorillonite and I/S clays at the centre and the top of the bentonite layer is estimated as 60 % and 45 % of the clay minerals respectively. There is a variation of illite content in the I/S clays, i.e., 41 - 65 % of I/S at the top and 36 - 51 % at the centre, which indicates that illitization was initiated from both the top and the bottom boundaries of the bentonite layer where potassium could enter.
3. Swelling pressure of the samples taken from the top and the centre of the clay layer was measured. The results indicated significant difference between the two, 3.8 MPa and 15 MPa respectively **[2]**. This implies that cementation of the clay due to precipitation of silicious substances proceeded to a greater extent at the top than the centre.

The original content of smectite is estimated to have been in the range of 60 - 80 % of the total mineral mass, and 75 % is regarded as a reasonably conservative estimate **[3]**.

2. Objectives

Silicification and illitization at elevated temperatures are considered to be potential degradation processes of the bentonite clay which is to be emplaced as a buffer material surrounding spent nuclear fuels in a deep underground repository. In this context, the geochemical evolution of the bentonite layers in Kinnekulle area can be regarded as a natural analogue to the possible chemical and physical processes in the future repositories.

A number of alternative conceptual models have been proposed by numerous researchers to explain loss of smectite and subsequent formation of illite observed in a number of natural systems. For simplicity, we may classify them into the following two groups;

1. solid state conversion from smectite to illite,
2. dissolution of smectite followed by precipitation (neoformation) of illite.

As for the Kinnekulle bentonite layer, based on the fact that the smectite is of low charge type, Pusch and Masden **[4]** have proposed the latter as the most likely conversion mechanism of smectite into illite and other minerals.

The objectives of the current modelling study are;

- to develop a number of reaction diffusion models corresponding to the solid state conversion model and the smectite dissolution model respectively,
- to apply the models to quantitatively reproduce the key features of the current mineralogy of the Kinnekulle bentonite described in Section 1,
- to compare results obtained by the two modelling options and evaluate their applicability to the silicification of Kinnekulle bentonite layer.

3. Model formulation

3.1 Geometry

We consider a planar one-dimensional geometry with co-ordinate x as depicted in Figure 1. We also set a fixed concentration boundary in the marine sediments 10 m away from the bentonite layer based on the information provided [3].

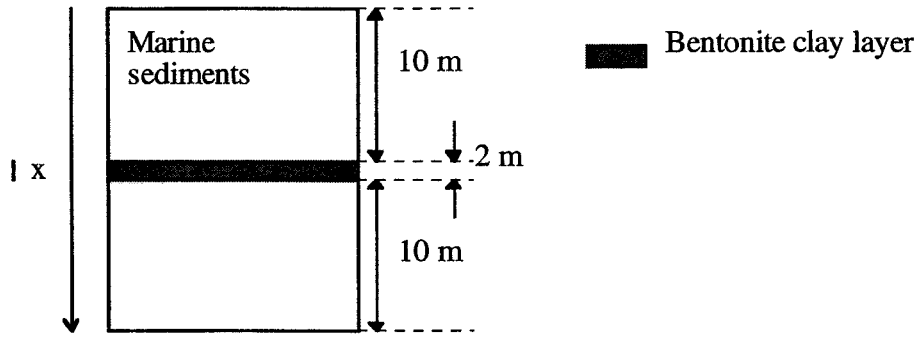

Figure 1: Modelled region

3.2 Reaction system

3.2.1 Aqueous species

Regarding $O_{10}(OH)_2$ as the unit, general formula for smectite and illite can be defined by $X_{0.35}Mg_{0.33}Al_{1.65}Si_4O_{10}(OH)_2$ and $K_{0.5-75}Al_{2.5-2.75}Si_{3.25-3.5}O_{10}(OH)_2$, where X is the interlayer, absorbed monovalent cation (Na^+ for the case of Na-montmorillonite) [5]. In reality, all the aqueous species associated with dissolution and precipitation of these two minerals participated, to certain extent, to the geochemical evolution of the Kinnekulle bentonite layer. However, for simplicity, we assume that concentration of H^+, Na^+ ,

Mg^{2+} and total Al in solution is conserved at the level in sea water and model only $SiO_{2(aq)}$ and K^+ for simplicity. This simplification seems to be justifiable as a starting point of the modelling exercise, taking into account; concentration of Na^+ and Mg^{2+} in the sea water is high anyway and it is unlikely for them to be further increased by dissolution (if any) of smectite to some significant extent; and pH and Al concentration are likely to be buffered by other minerals such as gibbsite **[5]**. Clearly validity of this assumption as well as its effect on the simulated silicification and illitization have to be checked. We address this issue in Section 5.

As for Al, however, we take into account temperature dependence of its speciation, namely the following reaction

(1) $$Al(OH)_4^- + 4\ H^+ = Al^{3+} + 4\ H_2O,$$

with log K taken from EQ3/6 data base **[6]** (see Table 2).

Both the initial concentration (everywhere in the modelled region) and boundary condition of $SiO_{2(aq)}$ in the marine sediment sufficiently far away from the bentonite layer are fixed at 1.0 e-4 mols/l which corresponds to equilibrium with respect to quartz at 25 C∞ (see 3.1.2). Considering the temperature rise which took place after the magmatic intrusion, it may be more reasonable to set $SiO_{2(aq)}$ to be in equilibrium at the given temperature. However, because of the distance from the clay layer where the reactions are most active, uncertainty in this aspect does not affect the results in the bentonite layer noticeably.

Initial and boundary concentration of K^+ were both fixed at 1.25 e-3 mols/l which was derived by substituting the pH equilibrated with montmorillonite in the sea water at 25 C∞* into a relationship of K^+ with H^+ in interstitial marine waters ($\log([K^+]/[H^+])\approx 5.5$ **[5]**.

*Remark

Derived from an EQ3/6 calculation.

3.2.2 Minerals

We model conversion of smectite into illite by the following two model options

Table 1 Aqueous species

Aqueous species	Initial and boundary conditions
$SiO_{2(aq)}$	1.0 e -4 (mols/l)
K^+	1.25 e -3 (mols/l)

Table 2 log K for Al speciation (1)

24.90 (273 K)
22.14 (298 K)
16.12 (333 K)
13.29 (373 K)
11.00 (423 K)
9.05 (473 K)

Solid state conversion

We assume that unit formula of smectite is converted into unit formula of illite for simplicity. Then, focusing on the aqueous species specified in the previous section and ignoring the rest, we have

(2) $$\text{smectite} + n_1K^+ = \text{illite} + n_2SiO_{2(aq)}\,.$$

The stoichiometric coefficients that appear in (2) can vary [5] but here, for simplicity, we set $n_1 = n_2 = 1$. Rate of the reaction (2) is given by

(3) $$R_1 = A\exp\left(\frac{-Ea}{RT}\right)[K^+]S^2,$$

where A; frequency factor (Table 3), Ea_1; activation energy (Table 3), R; gas constant, and S; fraction of smectite layers in the I/S.

Smectite dissolution

Here we split the process of smectite conversion to illite into dissolution of smectite and

precipitation of illite. As May *et.al.* have questioned whether it is possible for complex aluminosilicates of variable composition to reversibly equilibrate, a reliable "thermodynamic" data base for clay minerals is yet to be established. In particular, available quantitative knowledge concerning precipitation and "dissolution" of illite is limited. Hence, taking into account its structural similarity, we take muscovite as a representative to illite and obtain the following.

(4) $$Na_{0.33}\,Mg_{0.33}\,Al_{1.67}\,Si_4\,O_{10}\,(OH)_2 + 6H^+ = 0.33\,Na^+ + 0.33Mg^{2+} + 1.67Al^{3+} + 4\,SiO_{2(aq)} + 4\,H_2O,$$

(5) $$K\,AlSi_3\,O_{10}\,(OH)_2 + 10H^+ = K^+ + 3Al^{3+} + 3\,SiO_{2(aq)} + 6\,H_2O,$$

with logK as a function of temperature defined in Table 3 **[6]**.

As for the reaction rate, we use the following expressions obtained experimentally by Cama and Ayora **[7]** for reactions (4) and (5)

(6) $$R_i = \exp\left(\frac{-Ea}{RT}\right)\left(a_1\left[H^+\right]^{n_1} + a_2 + a_3\left[H^+\right]^{n_3}\right)S_A(s_1 + s_2)\left\{1-\left(\frac{Q}{K}\right)^b\right\}^p, \quad i = 2,3,$$

where a, b, n, p; constants (Table 3), S_A; specific surface area of the I/S, s_1, s_2; smectite and illite concentration, and Q ; solubility product defined according to (4) and (5) respectively. For the specific surface area of the clay, we use the data for compacted bentonite obtained in FEBEX programme **[11]**.

Initial content of smectite and illite are assumed to be 75 % of the total mineral* and 0 respectively.

Remark

We assume that density of water saturated clay is 2.1 [kg/l] and porosity is 0.35. This implies density of the clay itself is 2.7 [kg/l].

Other minerals

We also model precipitation and dissolution of quartz (s_3) and of amorphous silica (s_4)

(7) $$SiO_{2(c)} = SiO_{2(aq)},$$

(8) $$SiO_{2(am)} = SiO_{2(aq)},$$

with

(9) $$\log k = a_1 + a_2 T + \frac{a_3}{T},$$

where a; constants given in Table 3 **[8]**.

The reaction rate is expressed as the following form

(10) $$R_i = \begin{cases} k\left(1 - \frac{Q}{K}\right), & if\ s_i > 0, or\ Q > K, \\ 0, & otherwise \end{cases} \quad i = 4,5$$

and for k we have

(11) $$\log k = b_1 + b_2 T + \frac{b_3}{T},$$

where b; constants given in Table 3 **[8]**.

We assume that initial content of quartz and amorphous silica are 25 % of the total mineral and 0 respectively.

3.3 Reaction-diffusion equations

Based on the assumption that hydraulic conductivity of and head gradient across the bentonite layer and the adjacent marine sediments are sufficiently small, we only consider diffusion as the significant mass transport mechanism. The diffusion coefficient, D, has a temperature dependence and, by substituting temperature dependence of viscosity of pore water in a compacted bentonite experimentally measured by Chou **[9]** into the Einstein-Stokes formula, we have

(12) $$D(T) = \lambda(T - 260)T,$$

where constant λ is calibrated so that we have D = 1.0 e-8 m^2/s at 298 K.

Then, combining linear diffusion operators for aqueous species with the reaction rates defined in the previous section, we have the following system of semilinear parabolic equations

Table 3 Minerals

Reaction	Parameters for kinetics	Equilibrium constant
R_1: solid state conversion from smectite to illite (2)	Ea = 28 - 24 [kcal/mol] A = 8.08 e4 [M/s]	N/A
R_2: smectite reaction (4)	Ea = 15 [kcal/mol] $\log a_1$ = -5.0 $\log a_2$ = -13.6 $\log a_3$ = -14.7 n_1 = 0.38 n_3 = -0.22 n = 0.1 P = 13 S_A=600 [m^2/g]	logK= 3.55 (273 K) 2.48 (298 K) 0.43 (333 K) -1.79 (373 K) -4.16 (423 K) -6.16 (473 K)
R_3: illite (muscovite) reaction (5)	Ea = 15 [kcal/mol] $\log a_1$ = -11.4 $\log a_2$ = -12.8 $\log a_3$ = -15.0 n_1 = 0.38 n_3 = -0.22 n = 0.3 P=13 S_A=600 [m^2/g]	logK= 17.1 (273 K) 13.6 (298 K) 8.84 (333 K) 4.19 (373 K) -0.60 (423 K) -4.62 (473 K)
R_4: quartz reaction (7)	b_1 = 1.174 b_2 = -2.028 e-3 b_3 = 4158	a_1 = 1.881 a_2 = -2.028 e-3 a_3 = 1560
R_5: amorphous silica reaction (8)	b_1 = -0.369 b_2 = -7.889 e-4 b_3 = 3438	a_1 = 0.338 a_2 = -7.889 e-4 a_3 = 840.1

(13)

$$\frac{\partial u_1}{\partial t} = \nabla.(D(T)\nabla u_1) + (R_1) + 4(R_2) + 3(R_3) + R_4 + R_5,$$

$$\frac{\partial u_2}{\partial t} = \nabla.(D(T)\nabla u2) - (R_1) + (R_3),$$

$$\frac{\partial s_1}{\partial t} = -(R_1) - (R_2),$$

$$\frac{\partial s_2}{\partial t} = (R_1) - (R_3),$$

$$\frac{\partial s_3}{\partial t} = -R_4,$$

$$\frac{\partial s_4}{\partial t} = -R_5,$$

$$x \in [-10, 12], \quad t > 0$$

$$u_i(x,0) = u_{i0}, \quad x \in [-10, 12], \quad i = 1,2$$
$$s_j(x,0) = s_{j0}, \quad x \in [-10, 12], \quad j = 1,2,3,4$$
$$u_i(-10,t) = u_{i0}, \quad t > 0, \quad i = 1,2$$
$$u_i(12,t) = u_{i0}, \quad t > 0, \quad i = 1,2$$

where R_1 is considered only for the solid state conversion model, whereas R_2 and R_3 are considered only for the smectite dissolution model. Concentrations of both aqueous species and minerals are in (mass/litre of pore water).

3.4 Temperature field

The temperature evolution has been determined by use of conodont analysis and numerical calculations, assuming that the initial temperature of the diabase magma to be 1100 C∞ and applying some appropriate thermal properties for the sediment series **[1]** (see Figures 2 and 3 for temperature at the centre of the bentonite layer and average thermal gradient across the layer respectively). The temperature field at given time thus obtained are then digitised. We linearly interpolate this digitised temperature data and

defined $T(x,t)$, a continuous function of x and t. During the calculation, temperature at each node and each time step is referred to as $T(x,t)$.

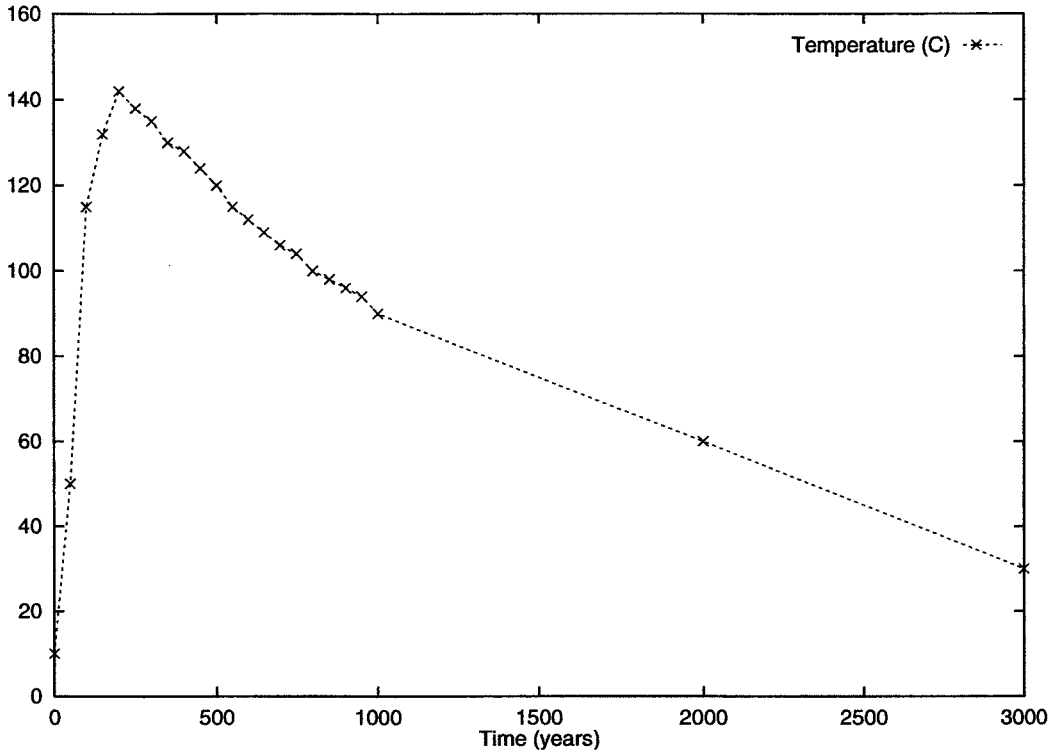

Figure 2: Evolution of temperature at the centre of the bentonite layer

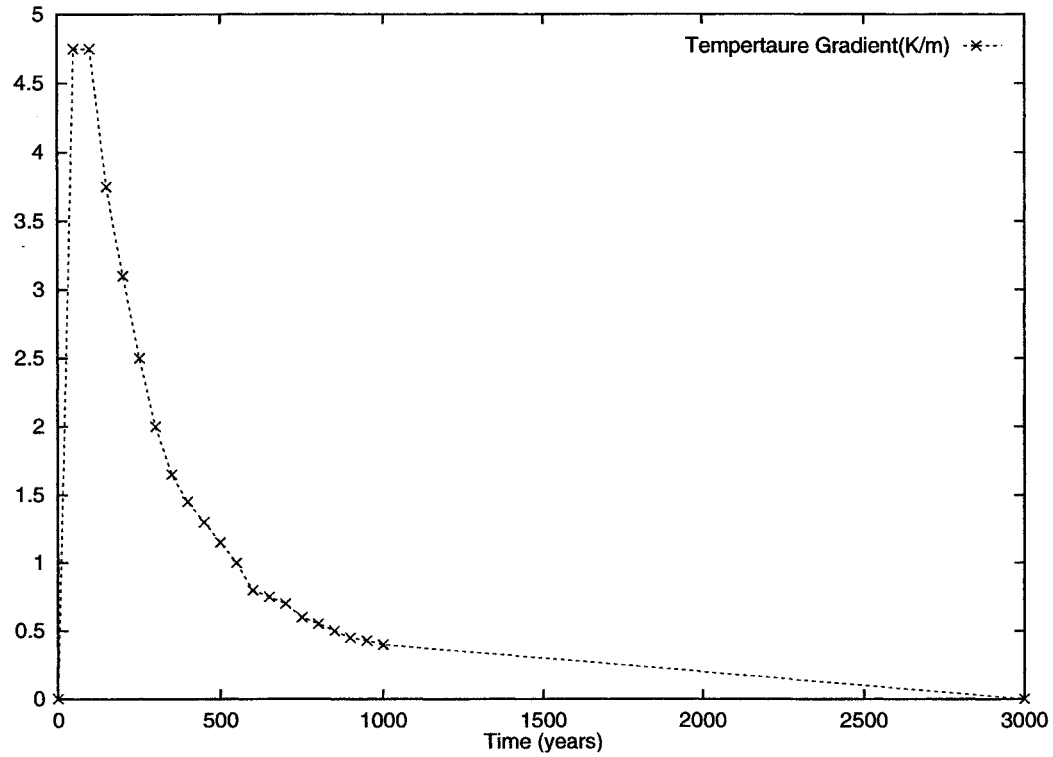

Figure 3: Evolution of average temperature gradient across the bentonite layer

4. Applications

Equations (3), (6), (9), (11), (12) and (13) form a system of DAEs (differential and algebraic equations). It is solved for the geometry given in Section 3.1 together with the initial and boundary conditions described in Section 3.2 by a general DAE solver, DYLAN **[10]**, which was developed by QuantiSci and is based on Gear's method.

4.1 Solid state conversion model

We carried out two calculations using the solid state conversion model with the activation energy E_a to be 28 kcal/mol and 24 kcal/mol respectively. The results are shown in Figures 4 to 17. The amount of illite formed after 3,000 years is small (0.012 weight % of total mineral for the case of E_a = 28 kcal/mol and 0.6 weight % for E_a = 24 kcal/mol) compared with maximal diffusive influx of potassium (calculated assuming potassium concentration in the clay layer to be 0), and we see relatively large precipitation at the centre of the clay layer as well. This implies that formation of illite in these cases are limited by the rate of the solid state conversion rather than the transport of potassium.

The amount of smectite lost is also small (0.01 weight % of total mineral for the case of E_a = 28 kcal/mol and 0.5 weight % for E_a = 24 kcal/mol) and this is consistent with the stoichiometry assumed in Section 3. In addition, because the smectite dissolution is small, amount of $SiO_{2(aq)}$ available for quartz and amorpshous silica precipitation is also limited. This resulted in only minor changes in quartz and effectively zero change in amorphous silica concentration after 3,000 years.

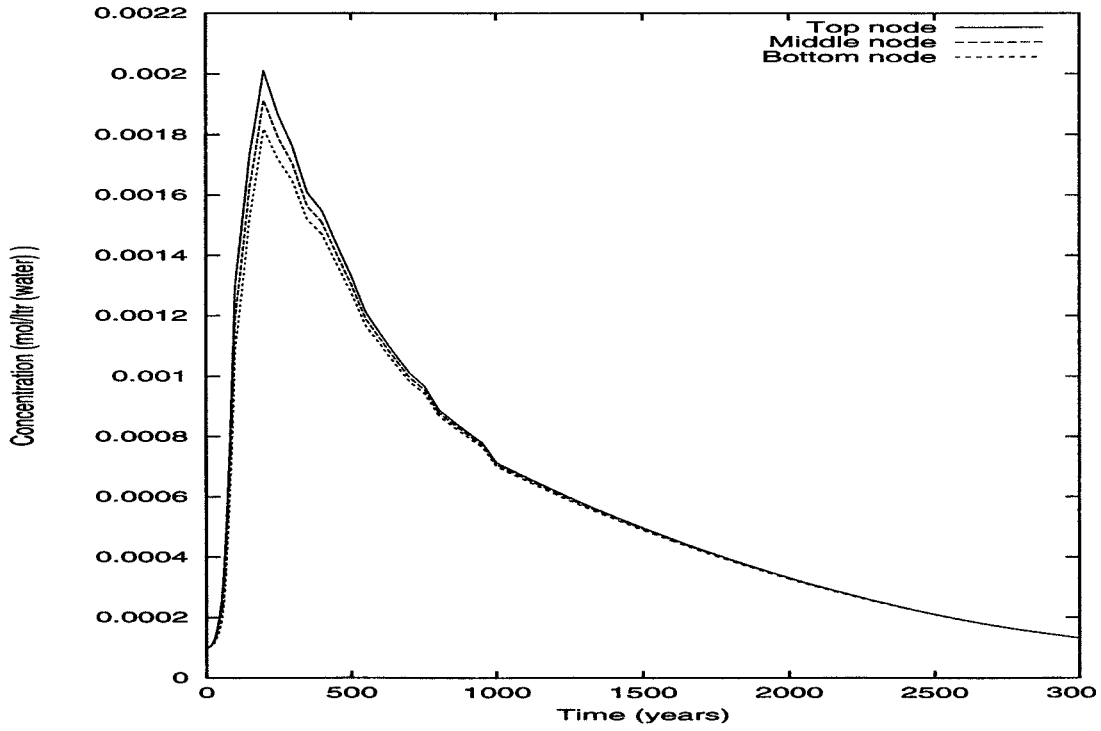

Figure 4: Evolution of $SiO_{2(aq)}$ concentration at the top, middle and bottom of the clay layer; solid state conversion model with activation energy = 28 kcal/mol.

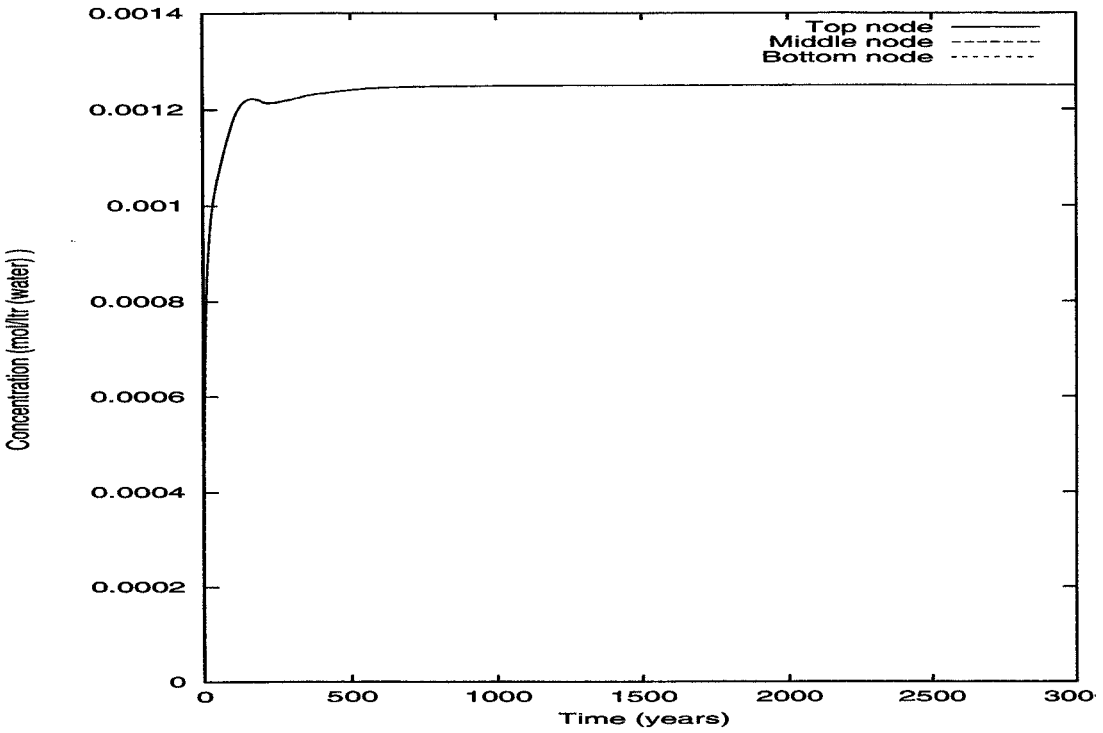

Figure 5: Evolution of potassium concentration at the top, middle and bottom of the clay layer; solid state conversion model with activation energy = 28 kcal/mol.

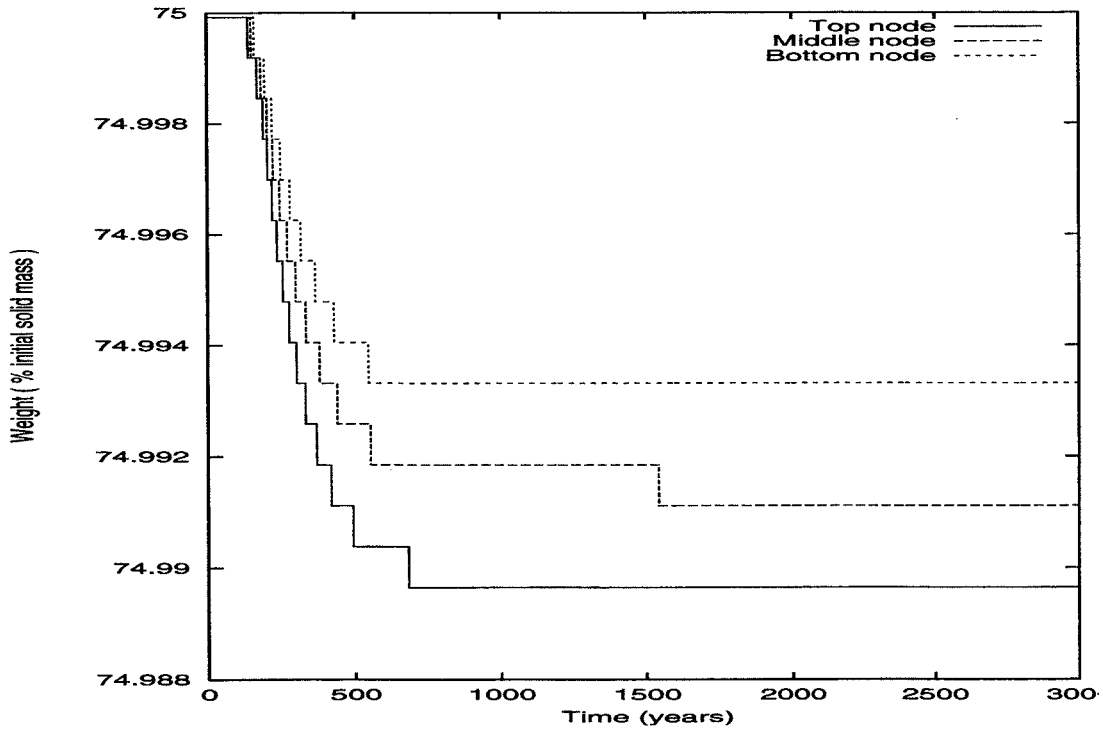

Figure 6: Evolution of smectite content at the top, middle and bottom of the clay layer; solid state conversion model with activation energy = 28 kcal/mol.

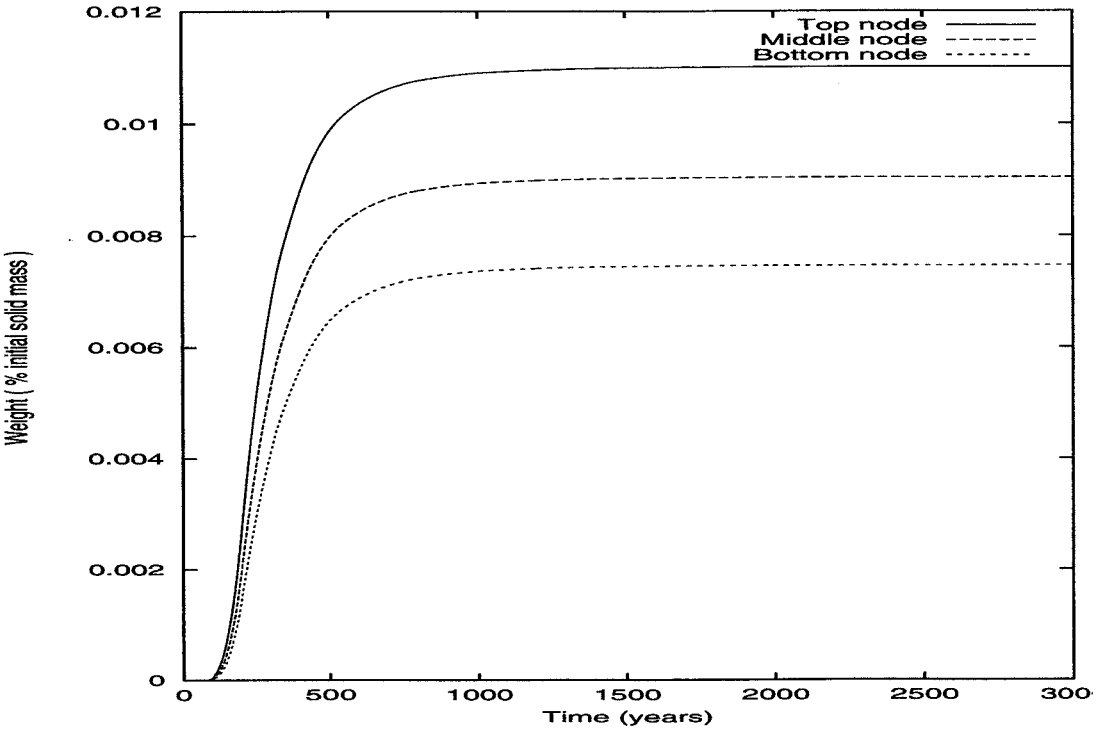

Figure 7: Evolution of illite content at the top, middle and bottom of the clay layer; solid state conversion model with activation energy = 28 kcal/mol.

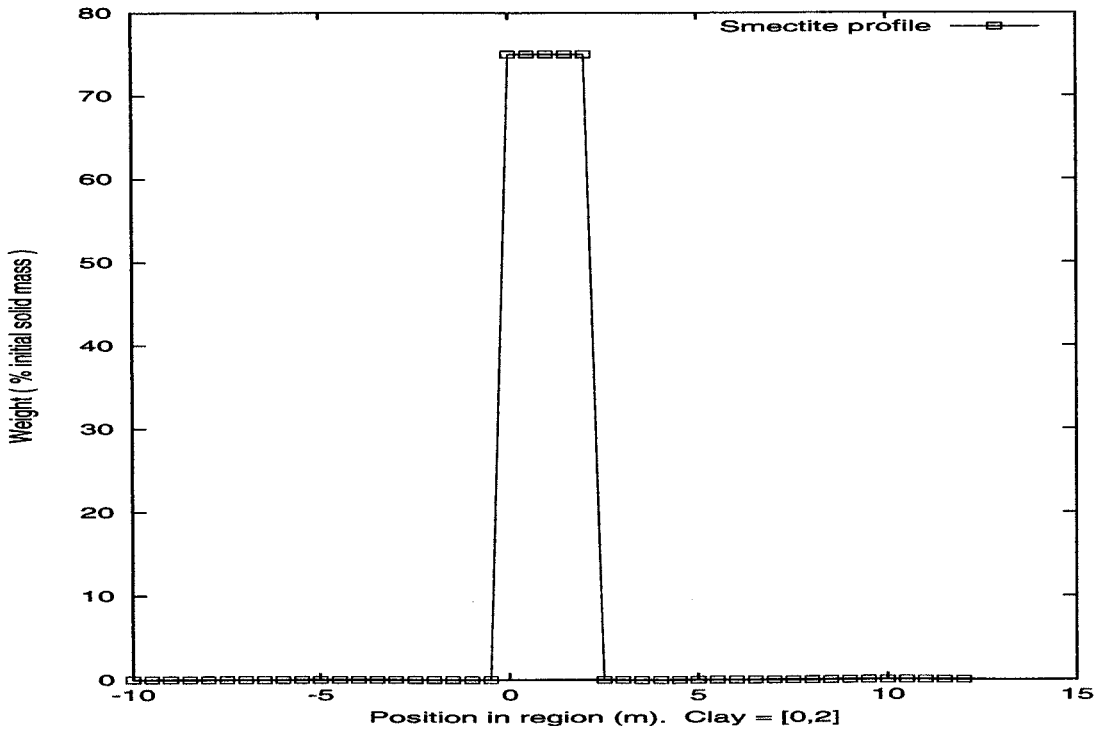

Figure 8: Final smectite content; solid state conversion model with activation energy = 28 kcal/mol

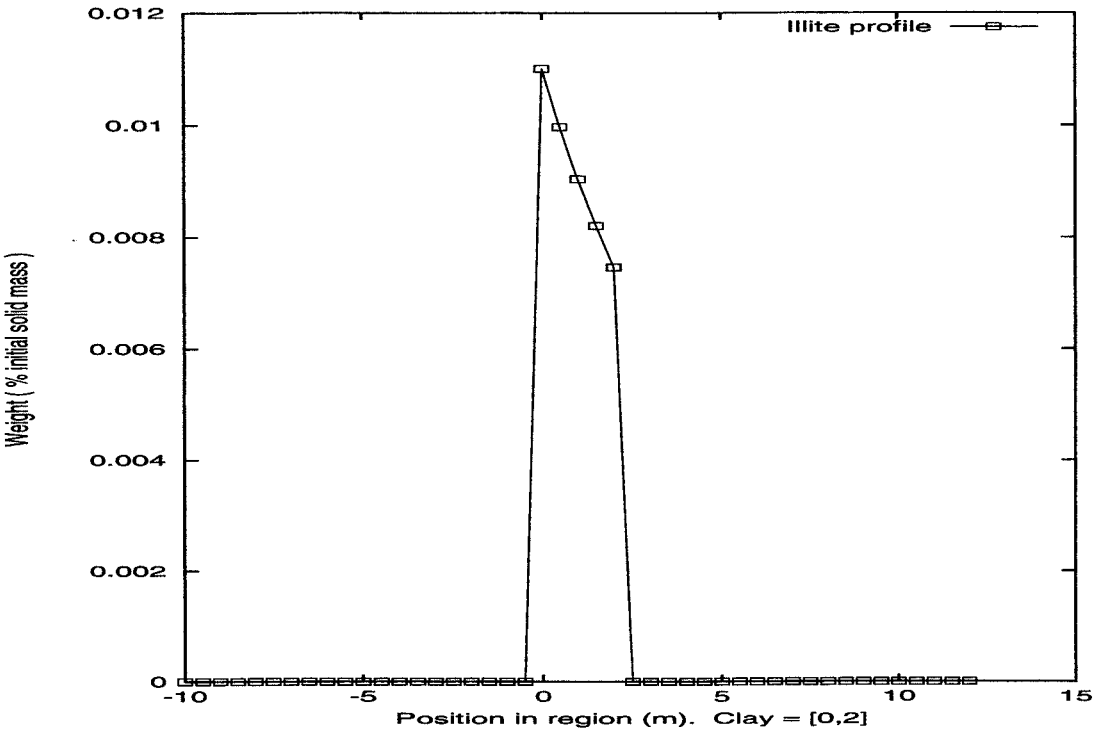

Figure 9: Final illite content; solid state conversion model with activation energy = 28 kcal/mol.

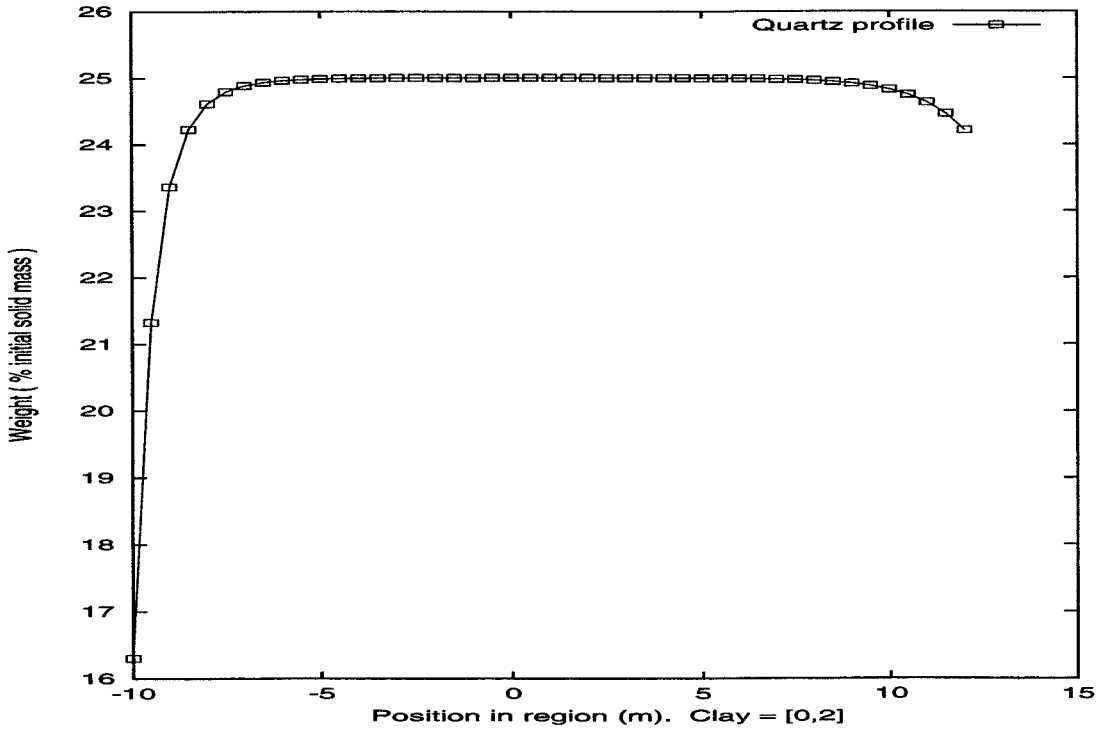

Figure 10: Final quartz content; solid state conversion model with activation energy = 28 kcal/mol.

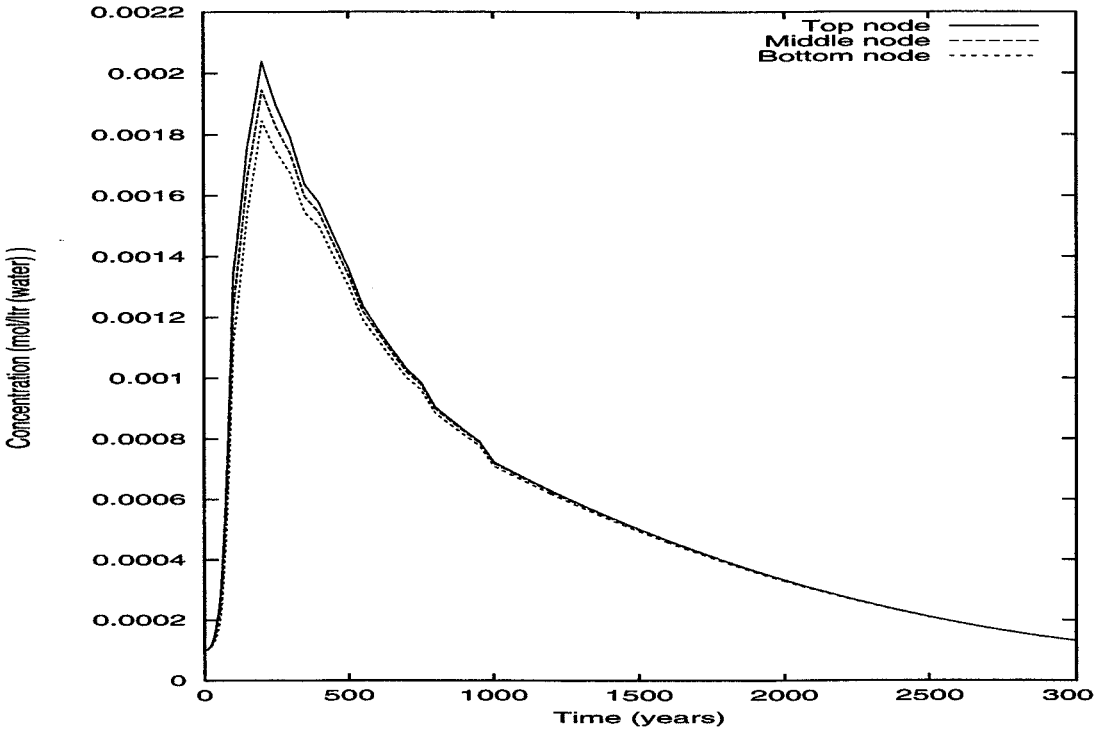

Figure 11: Evolution of $SiO_{2(aq)}$ concentration at the top, middle and bottom of the clay layer; solid state conversion model with activation energy = 24 kcal/mol.

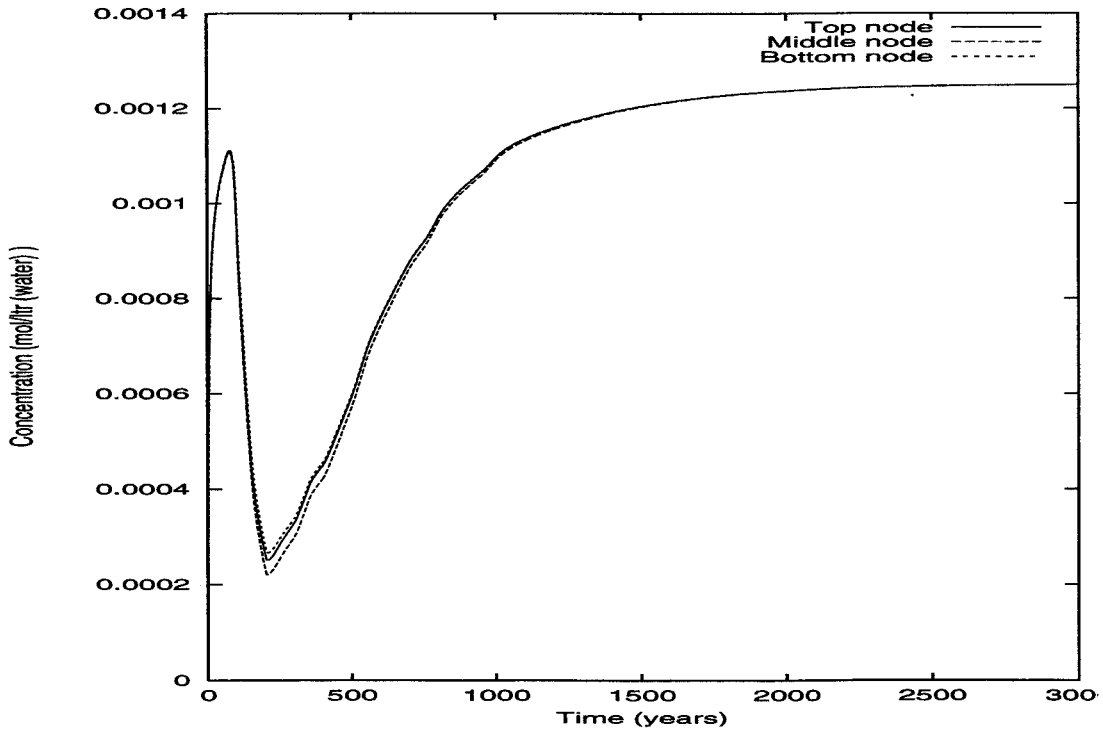

Figure 12: Evolution of potassium concentration at the top, middle and bottom of the clay layer; solid state conversion model with activation energy = 24 kcal/mol.

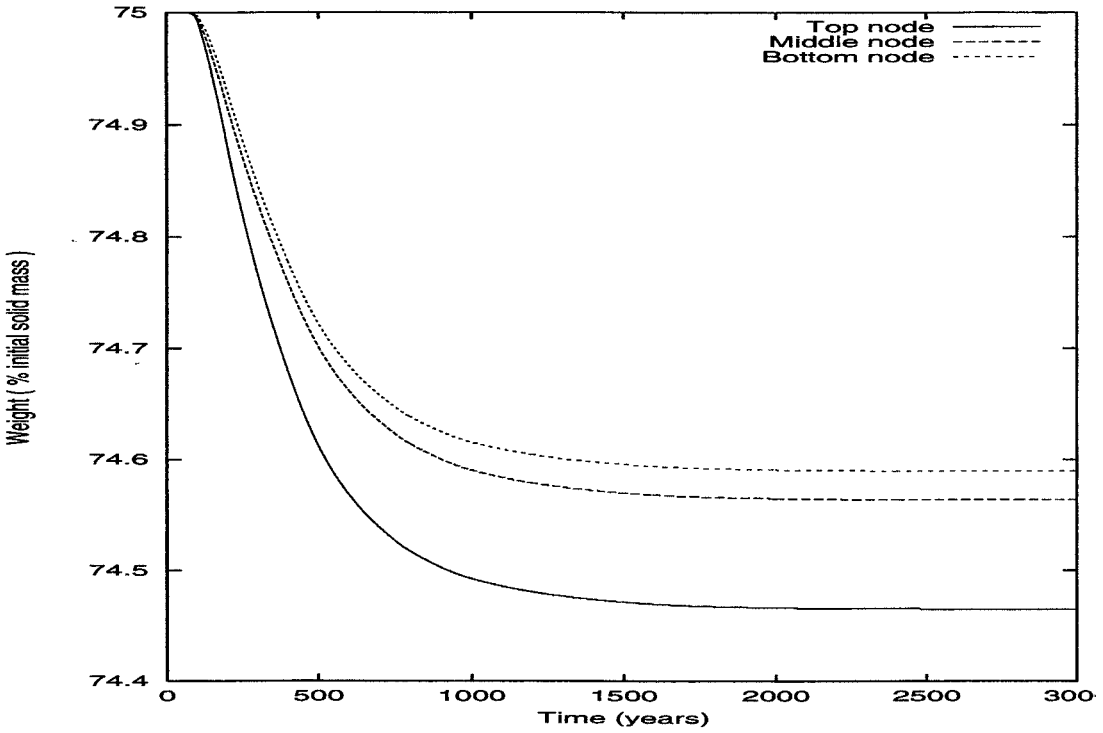

Figure 13: Evolution of smectite content at the top, middle and bottom of the clay layer; solid state conversion model with activation energy = 24 kcal/mol.

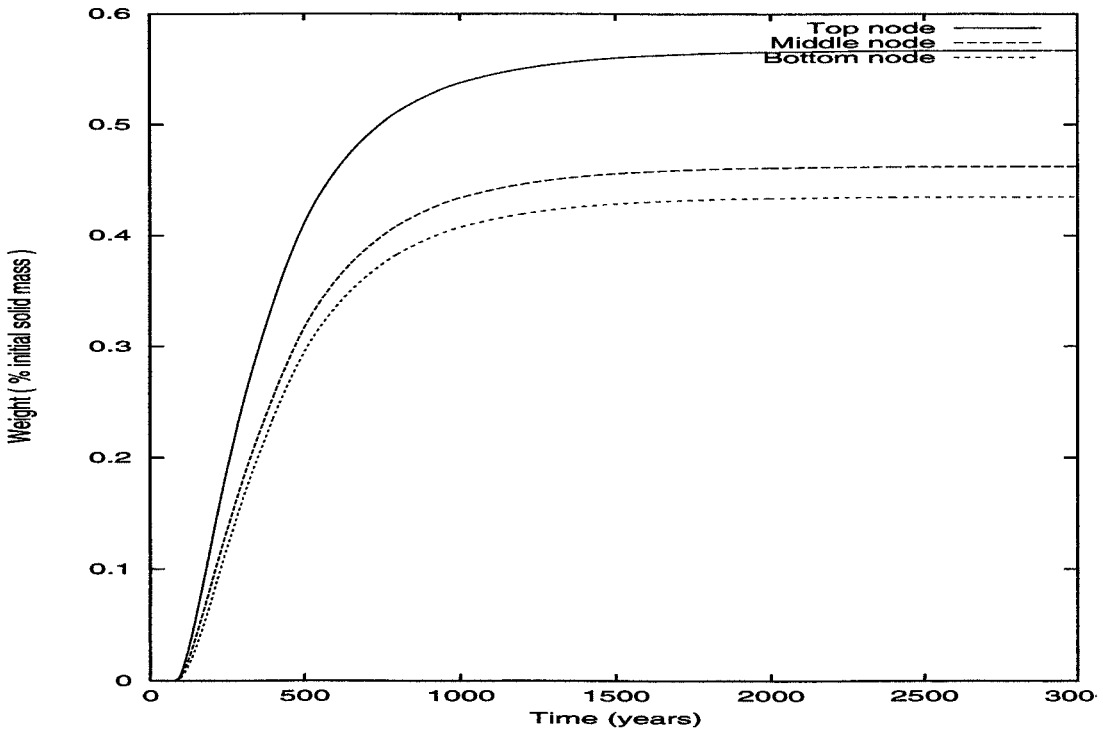

Figure 14: Evolution of illite content at the top, middle and bottom of the clay layer; solid state conversion model with activation energy = 24 kcal/mol.

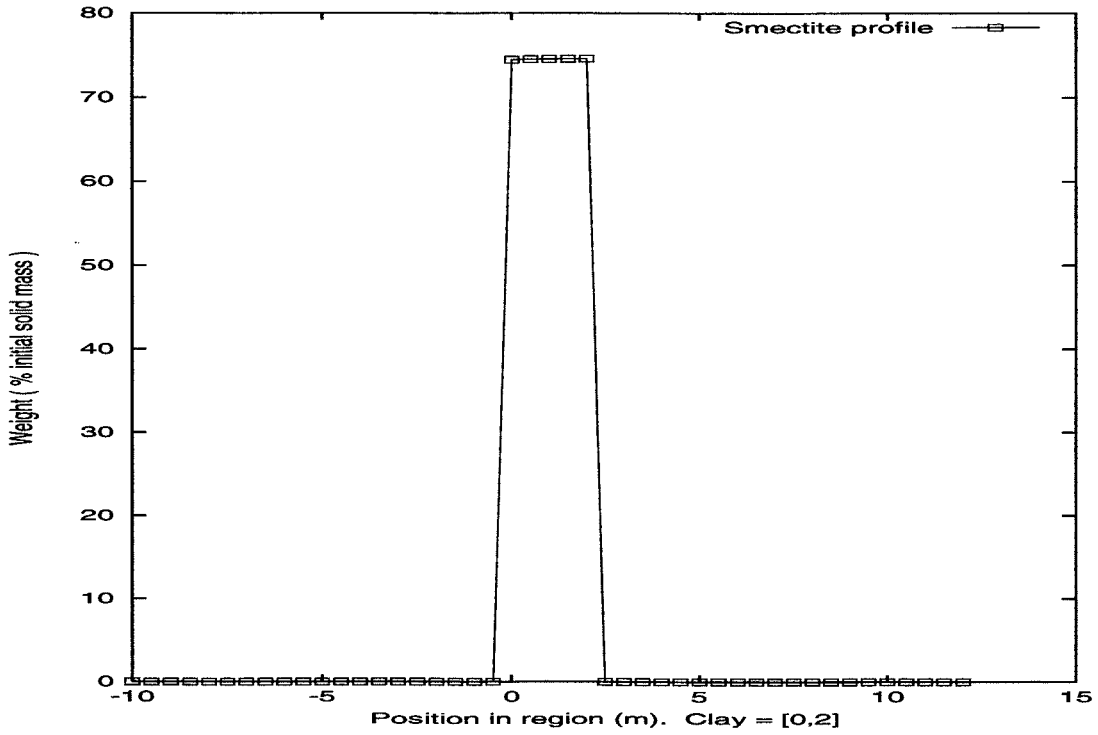

Figure 15: Final smectite content; solid state conversion model with activation energy = 24 kcal/mol.

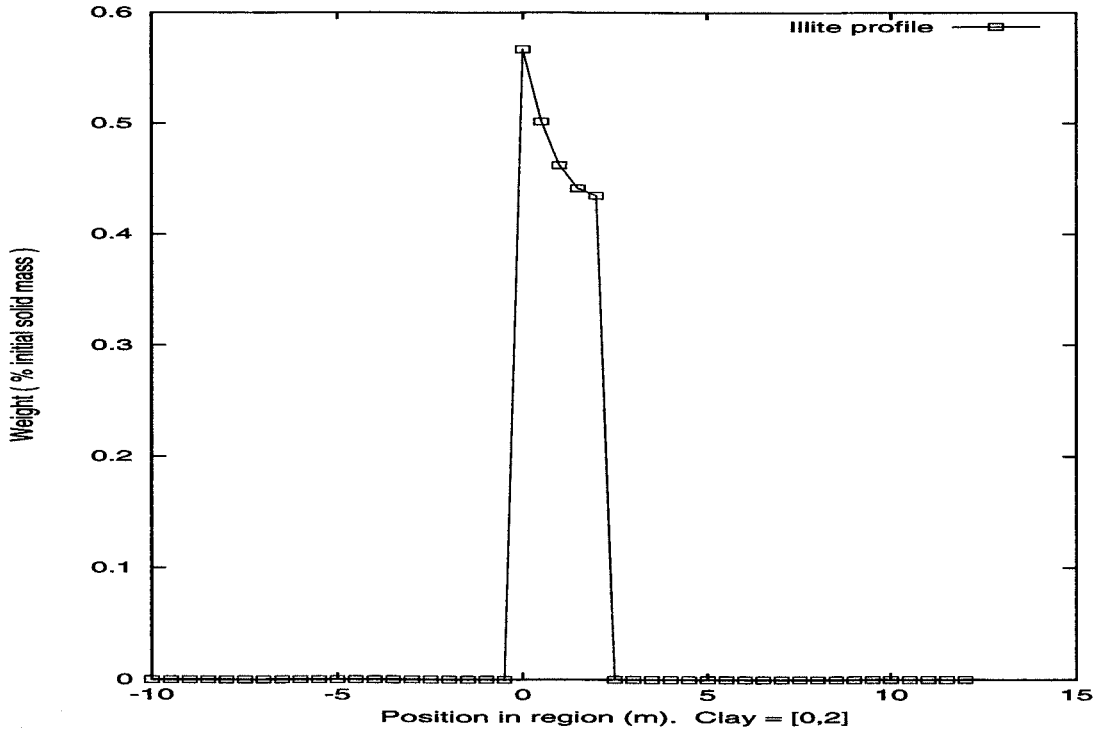

Figure 16: Final illite content; solid state conversion model with activation energy = 24 kcal/mol.

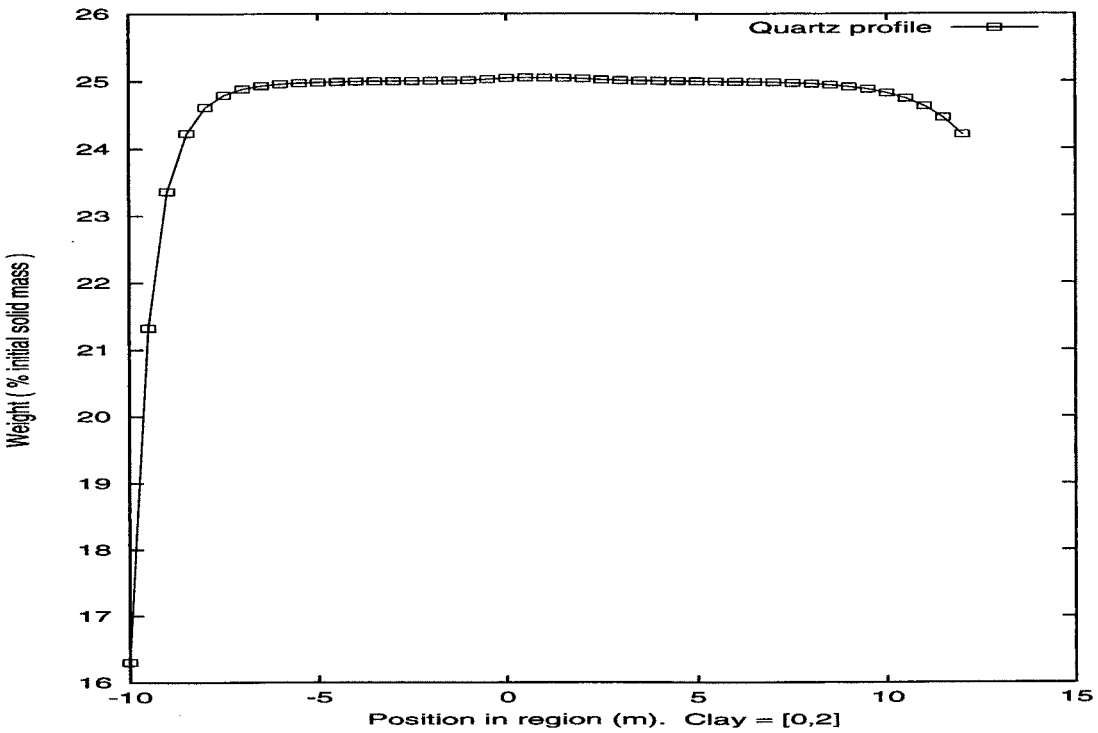

Figure 17: Final quartz content; solid state conversion model with activation energy = 24 kcal/mol.

4.2 Smectite dissolution model

We conducted a number of simulations using the model option assuming smectite dissolution (reaction (4)) described in Section 3. The result is summarised in Figures 18 to 21. Unlike the solid state conversion model, dissolution of smectite takes place to significant extent i.e., around 20 weight % (of total mineral) decrease of smectite as an average over the top 0.5 m segment of the bentonite layer and 7 weight % at the middle. The aqueous SiO_2 concentration profile in the bentonite layer is significantly higher than in the marine sediments while the temperature is above 100 °C due to dissolution of smectite. This excess SiO_2 in solution is consumed by diffusion into the sediments and precipitation of quartz. Quartz content at the top of the bentonite layer was more than 30 weight % after 3,000 years. No significant amount of amorphous silica was formed. Furthermore we observed that the aqueous SiO_2 concentration was in equilibrium with respect to the smectite reaction in the bentonite layer while the temperature is higher than 100 °C. This implies that loss of excess SiO_2 in solution due to diffusion is very much localised at the interface between the bentonite layer and the marine sediments and, thence, smectite dissolution at the top and the bottom of the bentonite layer is greater than

elsewhere. We performed a more detailed computation at the interface and found that average smectite content in the top 0.1 m and the bottom 0.1 m segments of the clay layer went down to 36 and 44 weight % of total mineral respectively after 3,000 years.

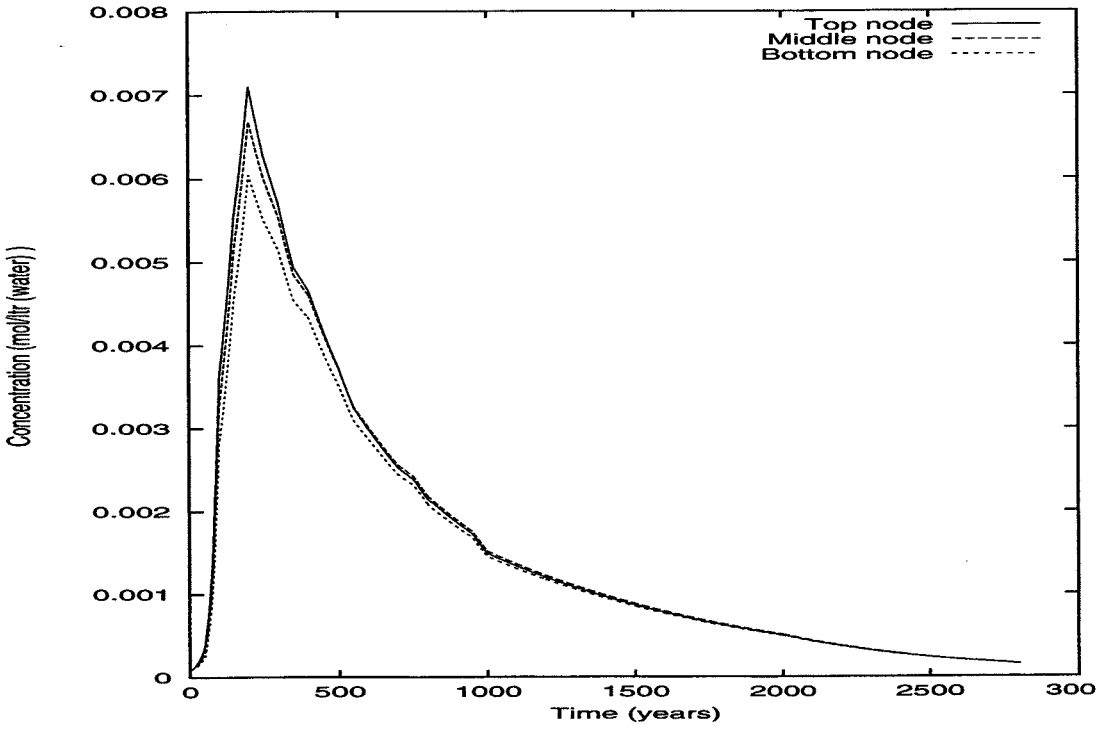

Figure 18: Evolution of $SiO_{2(aq)}$ concentration at the top, middle and bottom of the clay layer; smectite dissolution with reversible illite formation.

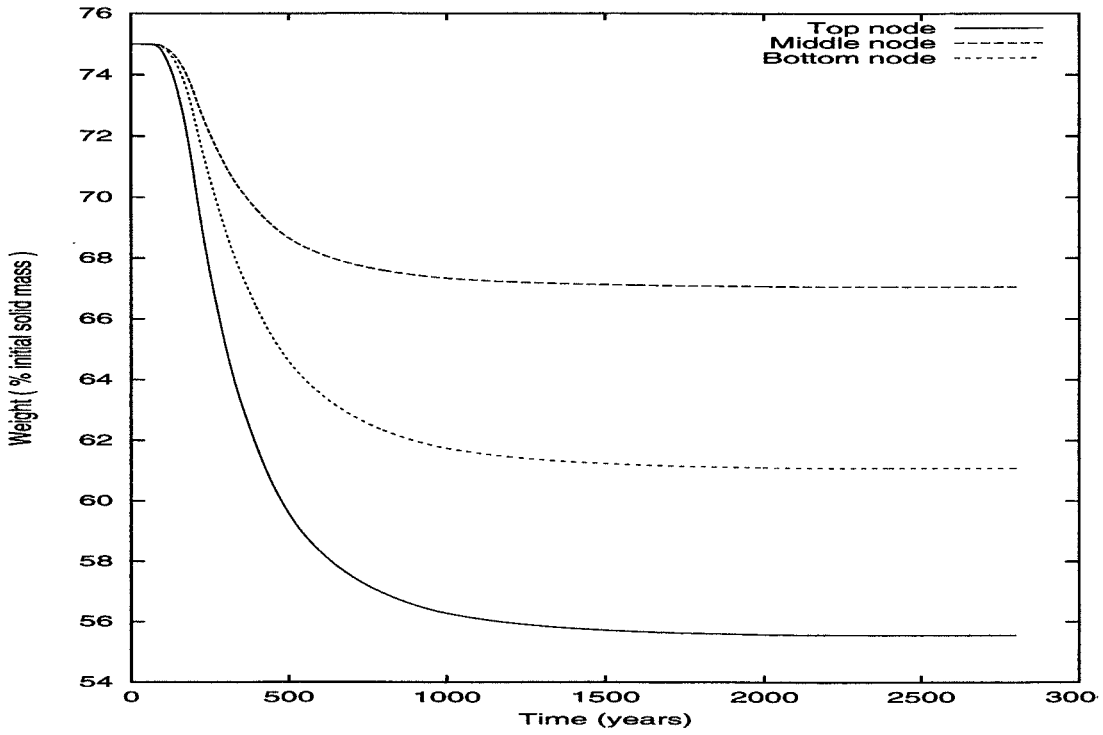

Figure 19: Evolution of smectite content at the top, middle and bottom of the clay layer; smectite dissolution with reversible illite formation.

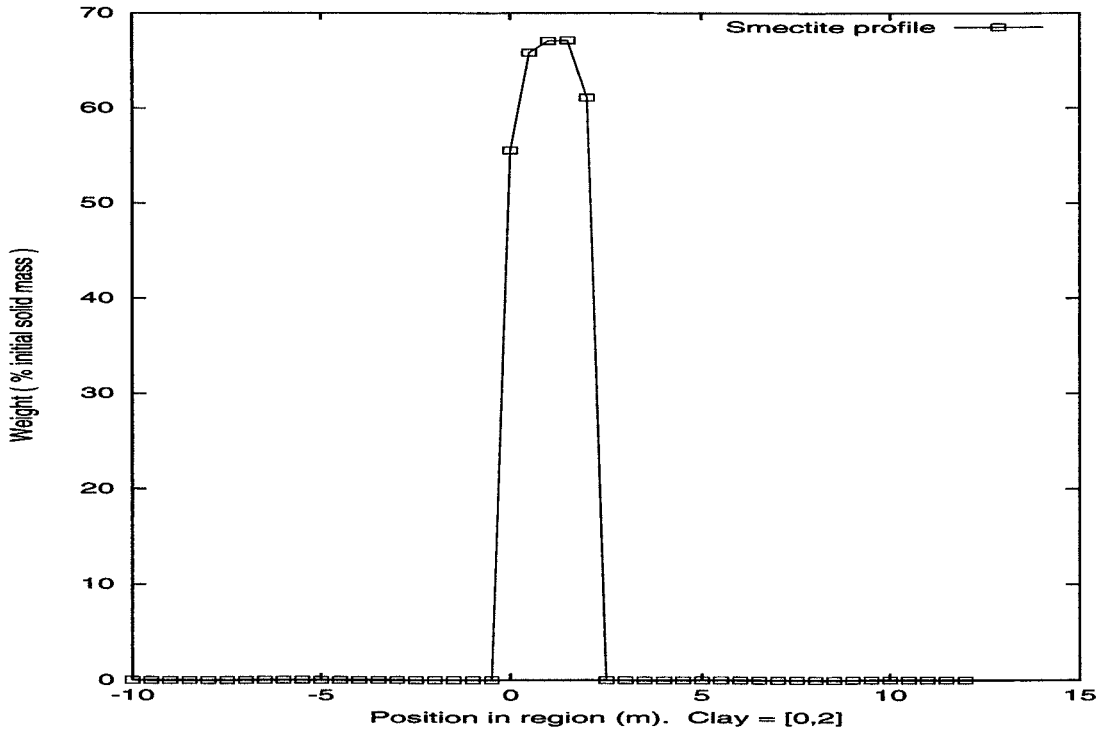

Figure 20: Final smectite content; smectite dissolution with reversible illite formation.

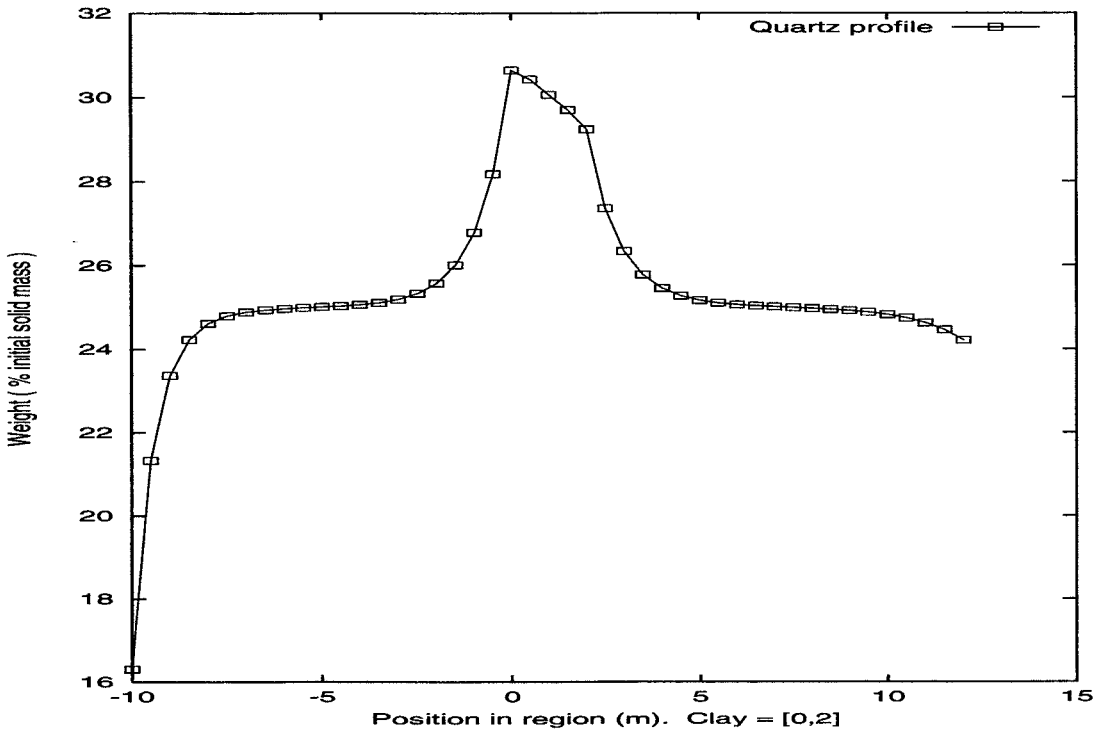

Figure 21: Final quartz content; smectite dissolution with reversible illite formation.

As for illite, however, we found no significant precipitation after 3,000 years. This is because reaction (5) stays undersaturated while temperature is high. It eventually gets supersaturated when the system cools down but the reaction rate constant at low temperature is too small to produce any noticeable amount of illite. We tried an alternative case with the illite equilibrium constant in EQ3/6 data base (instead of muscovite) coupled with the muscovite kinetics found in the experiments (because of lack of data for illite) but the result was very similar.

The fact that the simulations using smectite dissolution model coupled with the reversible illite precipitation model (reaction (5)) failed to explain the present illite content in the bentonite layer questions validity of reversible reaction model for illite formation. As an alternative we tried a case where we consider the smectite dissolution (reaction (4)) coupled with an irreversible illite formation. For simplicity we formulate this irreversible illite formation using the same expression as in equation (3) with lower activation energy (= 15 kcal/mol). The result is depicted in Figures 22 to 28. Here we have about 5 % weight of initial total mass of illite formed after 3,000 years. The smectite content is about 5 weight % less than in the previous runs due to additional consumption of aqueous SiO_2 by illite formation. Distribution of illite is very much localised at the edges of the

bentonite layer. This suggests that rate of the formation of illite is limited by diffusion of potassium rather than the chemical reactions.

As described in Section 3, we fixed the total Al concentration in the current calculations. However this assumption can affect saturation indice of the smectite reaction and, thence, impact the results. In particular if we model transport of Al explicitly with smectite dissolution and illite formation, the reversible illite formation model may become supersaturated during the thermal period and form significant amount of illite. To see this effect and other possible impact related to other aqueous species it is strongly recommended to conduct more detailed modelling including comprehensive aqueous speciations and other relevant minerals, although this is beyond the scope of the current project.

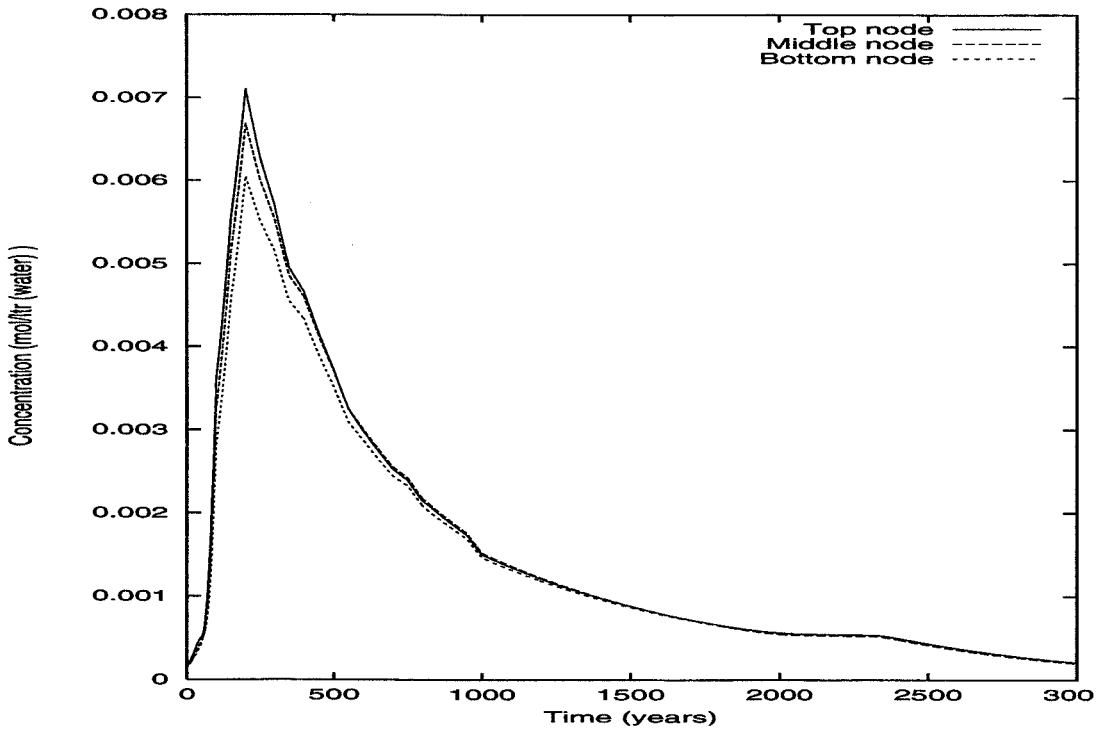

Figure 22: Evolution of $SiO_{2(aq)}$ concentration at the top, middle and bottom of the clay layer; smectite dissolution with irreversible illite formation.

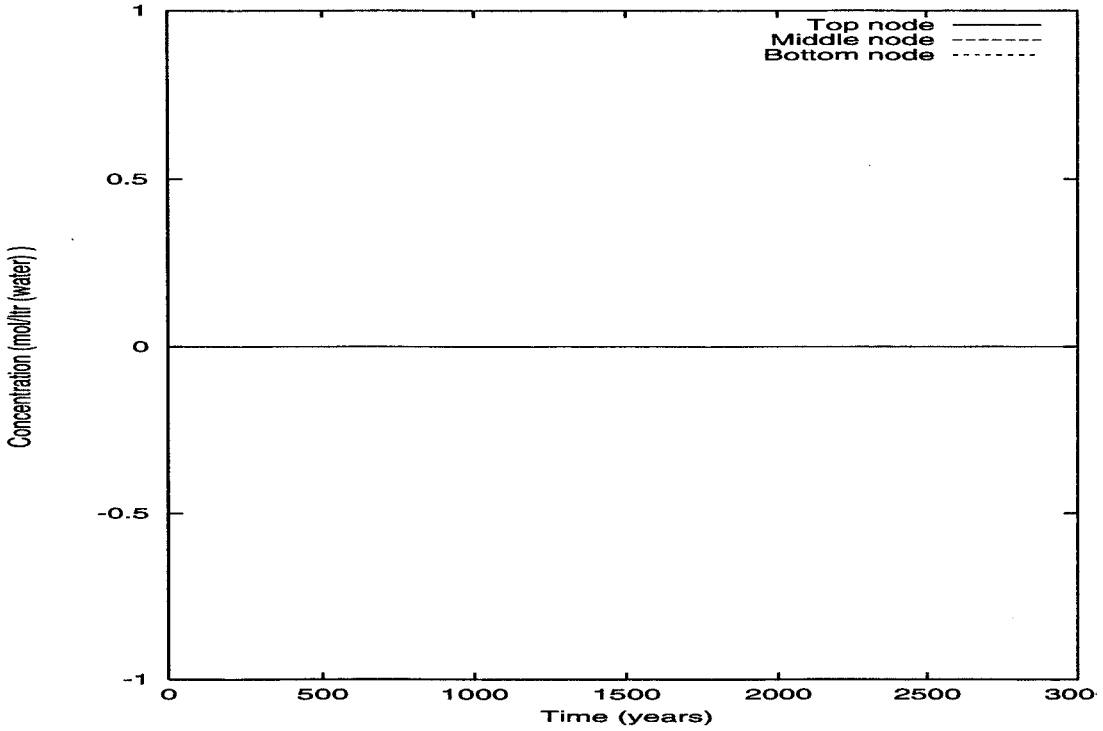

Figure 23: Evolution of potassium concentration at the top, middle and bottom of the clay layer; smectite dissolution with irreversible illite formation.

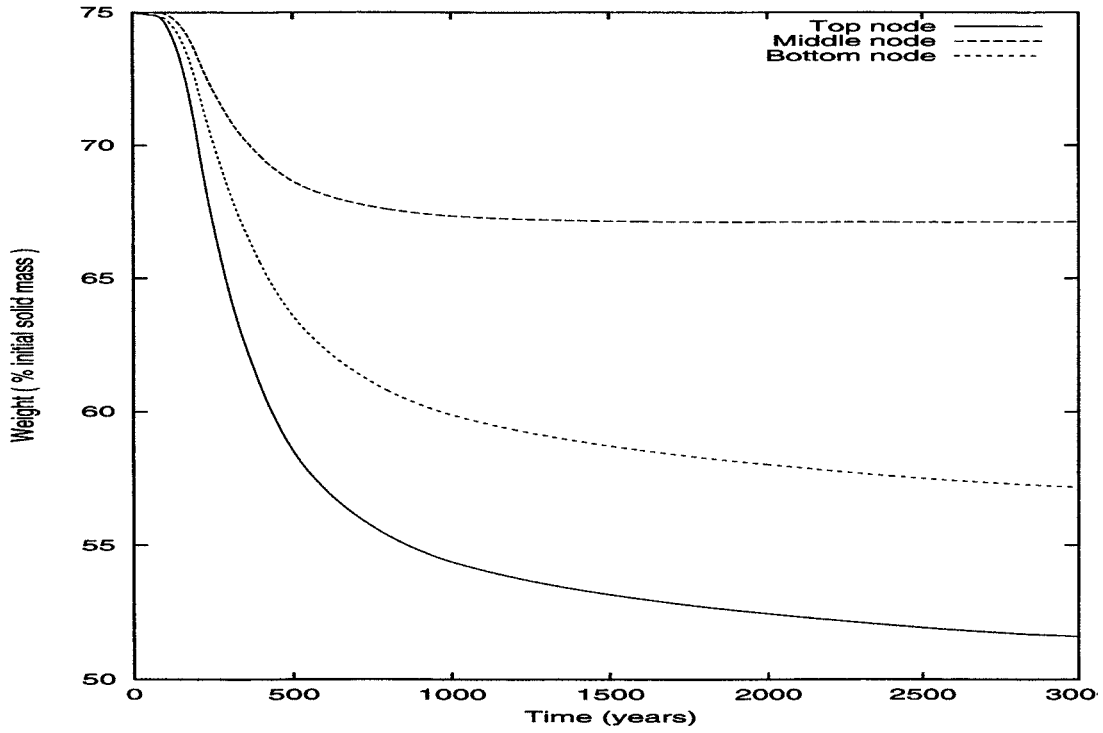

Figure 24: Evolution of smectite content at the top, middle and bottom of the clay layer; smectite dissolution with irreversible illite formation.

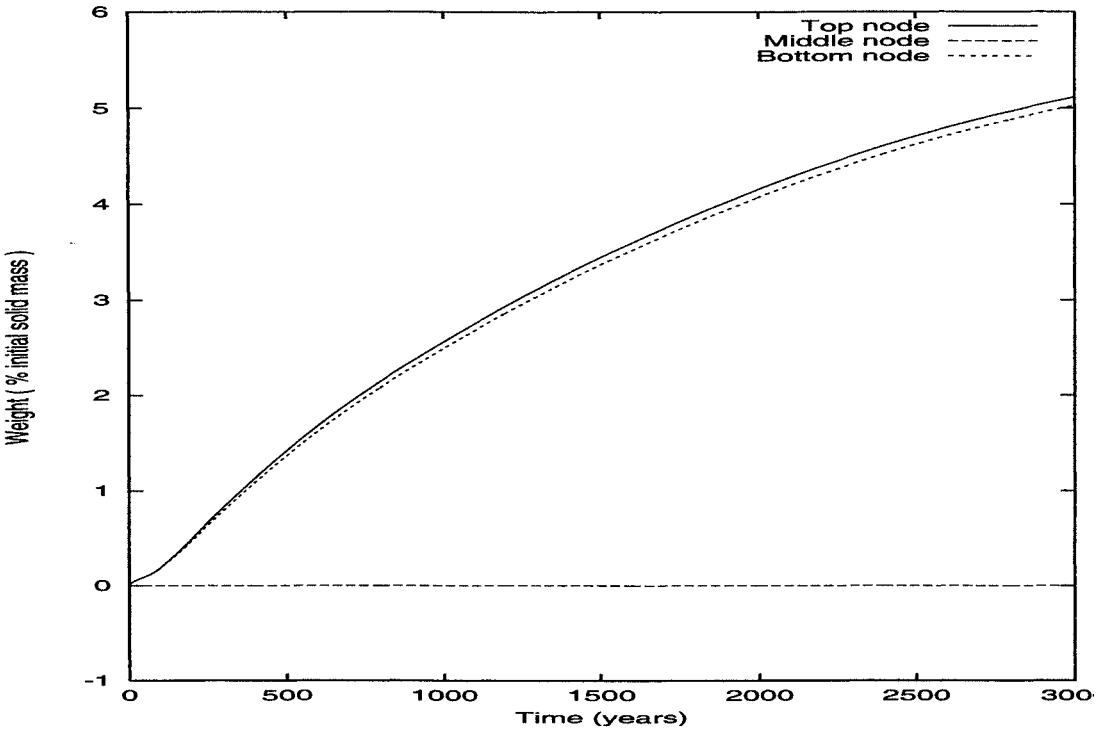

Figure 25: Evolution of illite content at the top, middle and bottom of the clay layer; smectite dissolution with irreversible illite formation.

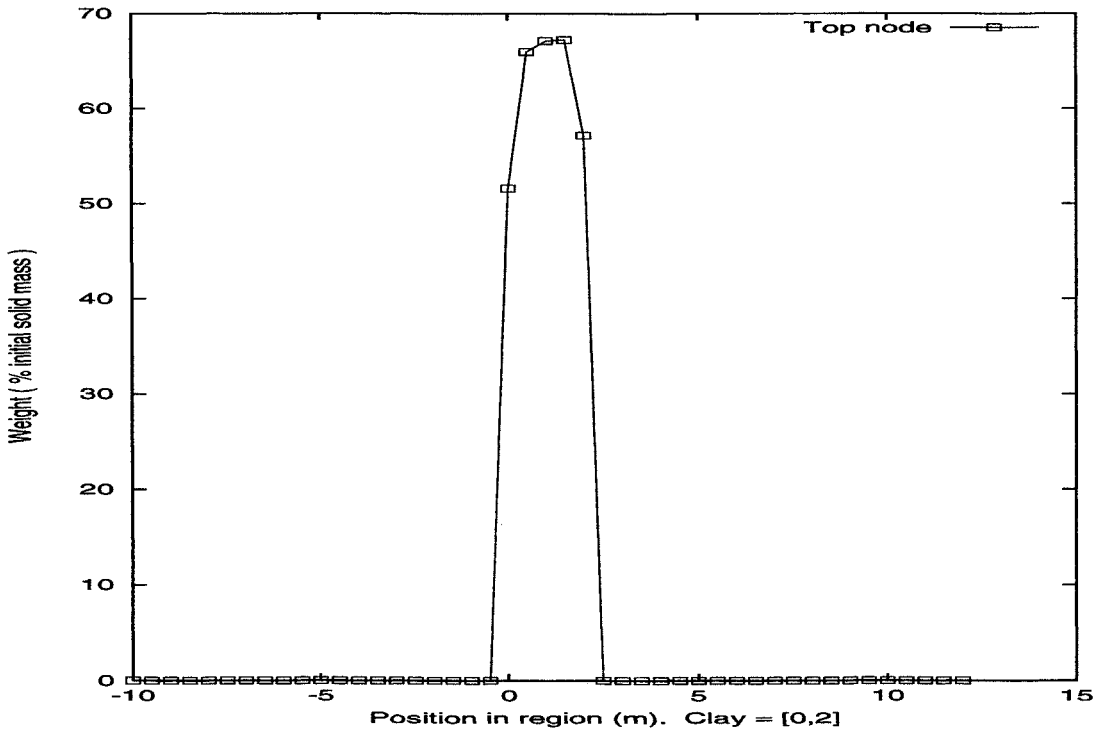

Figure 26: Final smectite content; smectite dissolution with irreversible illite formation.

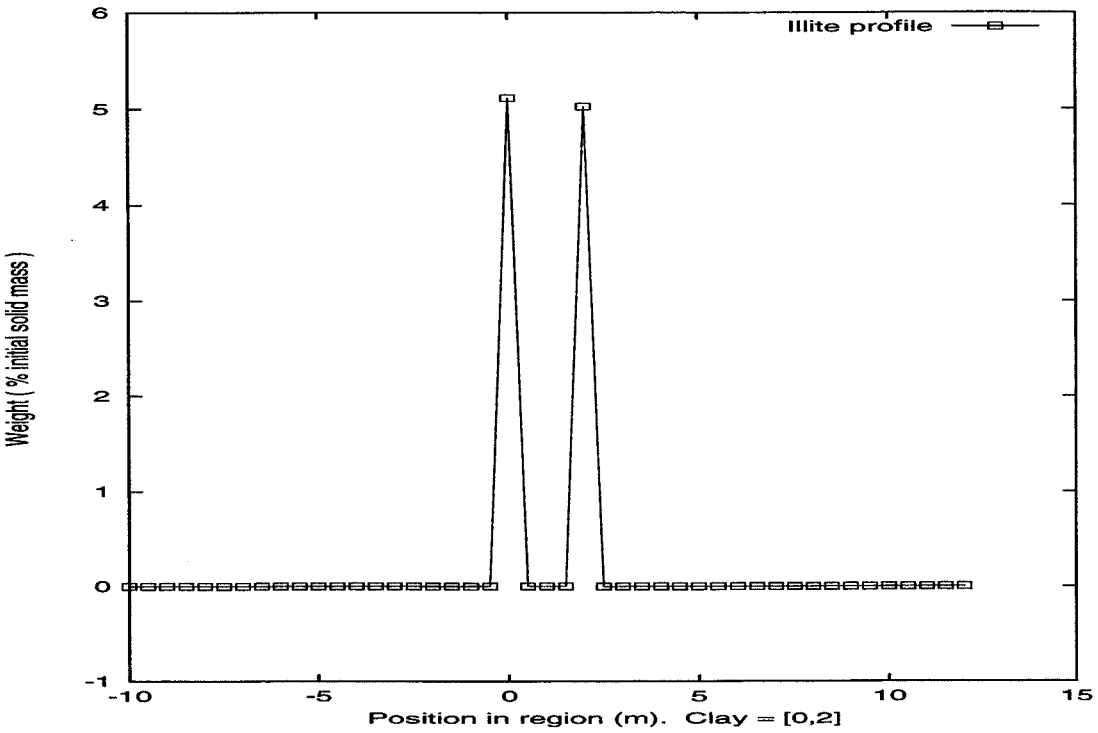

Figure 27: Final illite content; smectite dissolution with irreversible illite formation.

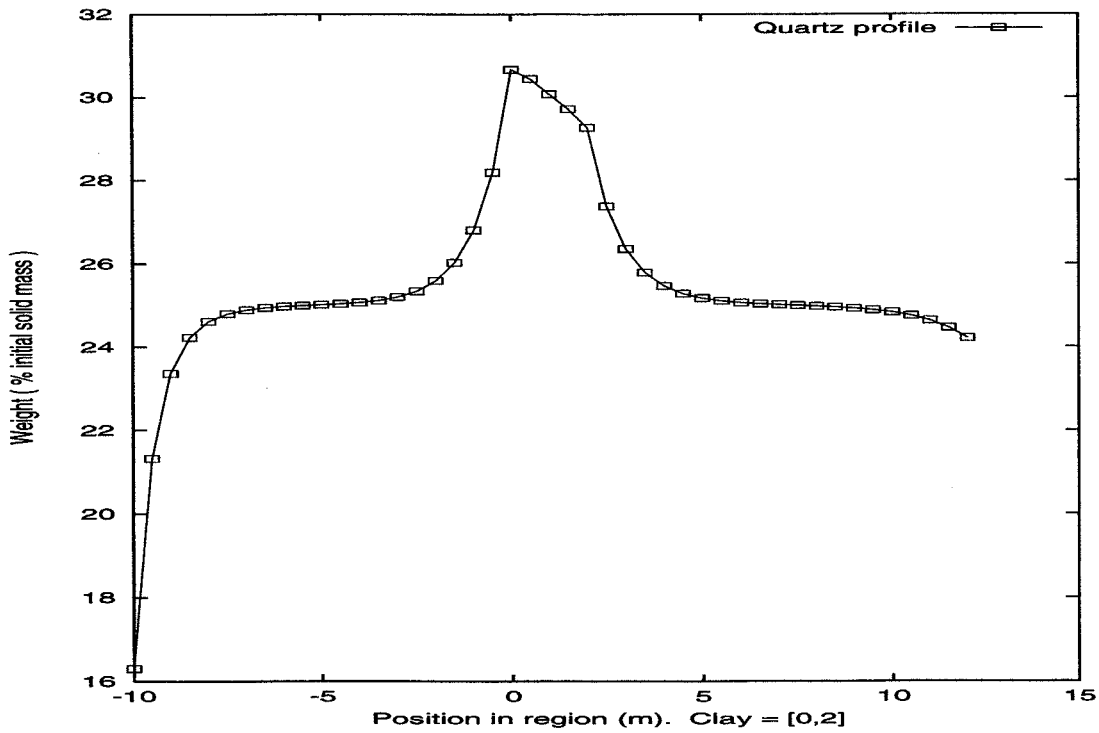

Figure 28: Final quartz content; smectite dissolution with irreversible illite formation.

5. Discussions

Two modelling options for conversion of smectite into illite, i.e., solid state conversion model and smectite dissolution model coupled with precipitation of illite, were applied to nonisothermal geochemical evolution of the bentonite layer at Kinnekulle. The solid state conversion model cannot explain the significant loss of the sum of the smectite and illite content which took place at Kinnekulle within the range of activation energies suggested in the literature , i.e., 28 to 24 kcal/mol. This implies that we need to consider an alternative mechanism for smectite consumption such as dissolution.

The smectite dissolution model which was derived by a series of experiments conducted as elevated temperatures, on the other hand, resulted in fair amount of decrease in the final smectite content after 3,000 years and proved to be a promising approach in this aspect. However the reversible precipitation/dissolution model employed in these first set of analyses revealed that the reaction stays undersaturated during the thermal period where we could have sufficiently fast reaction kinetics and that the current illite content cannot be explained by this type of model. A simple irreversible model for illite formation, which resembles the solid state conversion kinetics, illustrated the possibility of forming significant amount of illite mainly during the thermal period. This highlights neccessity of further research concerning detailed mechanism of the illite neoformation and its kinetics.

Maximal illite formation in the current case is constrained by diffusive transport of potassium, and this is somewhat smaller than the actual illite content observed in the site. This suggests that an alternative mechanism such as convection of pore water driven by the thermal gradient may have dominated transport. Underestimation of the cumulative smectite dissolution at the centre of the bentonite layer may also be explained by this factor. Another issue concerns the potassium concentration at the boundary which is set to be in the range observed in interstitial marine sediments in the current simulations. However this may have reached the level of the sea water and, also, the distance of the potassium concentration boundary from the clay layer may have been closer than 10 m. Thus another key issue for future research regards the spatial extent where the sea water and the groundwater in the marine sediment were mixed by thermal convection during the magmatic intrusion at Kinnekulle, and how it affected the flux of potassium into the clay layer.

Reference

[1] R. Pusch and P. Grindrod, *Chemical processes causing cementation in the Kinnekulle bentonites*, (1998)

[2] R. Pusch, L. Borgesson, M. Erlstrom, *Alteration of isolating properties of dense smectite clay in repository environment as exemplified by seven prequaternary clays*, SKB Technical Report TR 87-29 (1987)

[3] R. Pusch, Private communication, July 1998

[4] R. Pusch and T.F.Masden, Aspects of the illitization of the Kinnekulle bentonites, Clay and Clay Minerals, Vol.43, No.3, pp261 - 270 (1995)

[5] D. Langmuir, Aqueous environmental Geochemistry, Prentice Hall

[6] EQ3/6 data base

[7] J. Cama and C. Ayora, *Modelling the dissolution behaviour of a clayey barrier*, Proceedings of Goldschmidt Conference Toulouse 1998, pp 271 - 272

[8] S. Carroll, E. Mroczek, M. Alai and M. Ebert, *Amorpshous silica precipitation (60 C∞ to 120 C∞): Comparison of laboratory and field rates*, Geochemica et Cosmochimica Acta **Vol. 62** No. 8, pp 1379 - 1396 (1998)

[9] W.J.Chou, J.O.Lee and K.S.Chun, *Influence of temperature on hydraulic conductivity in compacted bentonite*, preprint (1997)

[10] J.Humm and P.C.Robinson, *DYLAN User's guide*, QuantiSci Technical Report (1998)

[11] enresa, FEBEX: *Full-scale engineered barriers experiment in crystalline host rock, Pre-operational stage summary report*, Publication Technica Num. 01/98 (1998)

List of SKB reports

Annual Reports

1977-78
TR 121
KBS Technical Reports 1 – 120
Summaries
Stockholm, May 1979

1979
TR 79-28
The KBS Annual Report 1979
KBS Technical Reports 79-01 – 79-27
Summaries
Stockholm, March 1980

1980
TR 80-26
The KBS Annual Report 1980
KBS Technical Reports 80-01 – 80-25
Summaries
Stockholm, March 1981

1981
TR 81-17
The KBS Annual Report 1981
KBS Technical Reports 81-01 – 81-16
Summaries
Stockholm, April 1982

1982
TR 82-28
The KBS Annual Report 1982
KBS Technical Reports 82-01 – 82-27
Summaries
Stockholm, July 1983

1983
TR 83-77
The KBS Annual Report 1983
KBS Technical Reports 83-01 – 83-76
Summaries
Stockholm, June 1984

1984
TR 85-01
Annual Research and Development Report 1984
Including Summaries of Technical Reports Issued during 1984. (Technical Reports 84-01 – 84-19)
Stockholm, June1985

1985
TR 85-20
Annual Research and Development Report 1985
Including Summaries of Technical Reports Issued during 1985. (Technical Reports 85-01 – 85-19)
Stockholm, May 1986

1986
TR 86-31
SKB Annual Report 1986
Including Summaries of Technical Reports Issued during 1986
Stockholm, May 1987

1987
TR 87-33
SKB Annual Report 1987
Including Summaries of Technical Reports Issued during 1987
Stockholm, May 1988

1988
TR 88-32
SKB Annual Report 1988
Including Summaries of Technical Reports Issued during 1988
Stockholm, May 1989

1989
TR 89-40
SKB Annual Report 1989
Including Summaries of Technical Reports Issued during 1989
Stockholm, May 1990

1990
TR 90-46
SKB Annual Report 1990
Including Summaries of Technical Reports Issued during 1990
Stockholm, May 1991

1991
TR 91-64
SKB Annual Report 1991
Including Summaries of Technical Reports Issued during 1991
Stockholm, April 1992

1992
TR 92-46
SKB Annual Report 1992
Including Summaries of Technical Reports Issued during 1992
Stockholm, May 1993

1993
TR 93-34
SKB Annual Report 1993
Including Summaries of Technical Reports Issued during 1993
Stockholm, May 1994

1994
TR 94-33
SKB Annual Report 1994
Including Summaries of Technical Reports Issued during 1994
Stockholm, May 1995

1995
TR 95-37
SKB Annual Report 1995
Including Summaries of Technical Reports Issued during 1995
Stockholm, May 1996

1996
TR 96-25
SKB Annual Report 1996
Including Summaries of Technical Reports Issued during 1996
Stockholm, May 1997

List of SKB Technical Reports 1998

TR 98-01
Global thermo-mechanical effects from a KBS-3 type repository. Summary report
Eva Hakami, Stig-Olof Olofsson, Hossein Hakami, Jan Israelsson
Itasca Geomekanik AB, Stockholm, Sweden
April 1998

TR 98-02
Parameters of importance to determine during geoscientific site investigation
Johan Andersson[1], Karl-Erik Almén[2], Lars O Ericsson[3], Anders Fredriksson[4], Fred Karlsson[3], Roy Stanfors[5], Anders Ström[3]
[1] QuantiSci AB
[2] KEA GEO-Konsult AB
[3] SKB
[4] ADG Grundteknik KB
[5] Roy Stanfors Consulting AB
June 1998

TR 98-03
Summary of hydrochemical conditions at Aberg, Beberg and Ceberg
Marcus Laaksoharju, Iona Gurban, Christina Skårman
Intera KB
May 1998

TR 98-04
Maqarin Natural Analogue Study: Phase III
J A T Smellie (ed.)
Conterra AB
September 1998

TR 98-05
The Very Deep Hole Concept – Geoscientific appraisal of conditions at great depth
C Juhlin[1], T Wallroth[2], J Smellie[3], T Eliasson[4], C Ljunggren[5], B Leijon[3], J Beswick[6]
[1] Christopher Juhlin Consulting
[2] Bergab Consulting Geologists
[3] Conterra AB
[4] Geological Survey of Sweden
[5] Vattenfall Hydropower AB
[6] EDECO Petroleum Services Ltd.
June 1998

TR 98-06
Indications of uranium transport around the reactor zone at Bagombe (Oklo)
I Gurban[1], M Laaksoharju[1], E Ledoux[2], B Made[2], A L Salignac[2],
[1] Intera KB, Stockholm, Sweden
[2] Ecole des Mines, Paris, France
August 1998

TR 98-07
PLAN 98 – Costs for management of the radioactive waste from nuclear power production
Swedish Nuclear Fuel and Waste Management Co
June 1998

TR 98-08
Design premises for canister for spent nuclear fuel
Lars Werme
Svensk Kärnbränslehantering AB
September 1998

TR 98-09
Test manufacturing of copper canisters with cast inserts Assessment report
Claes-Göran Andersson
Svensk Kärnbränslehantering AB
Augusti 1998

TR 98-22

Development of a kinetic model for the dissolution of the UO_2 spent nuclear fuel

Application of the model to the minor radionuclides

Jordi Bruno, Esther Cera, Lara Duro, Jordi Pon
QuantiSci SL, Barcelona, Spain
Joan de Pablo
Department Enginyeria Quimica, UPC, Barcelona, Spain
Trygve Eriksen
Department Nuclear Chemistry, KTH, Stockholm
May 1998

TR 98-23

Site-scale groundwater flow modelling of Aberg

Douglas Walker
Duke Engineering & Services
Björn Gylling
Kemakta Konsult AB
December 1998

TR 98-24

Investigation of the large scale regional hydrogeological situation at Beberg

Lee Hartley
AEA Technology, UK
Anders Boghammar, Bertil Grundfelt
Kemakta Konsult AB
December 1998

ISSN 0284-3757
CM Gruppen AB, Bromma, 1999